

Re and Tc Complexes with Pyrazolyl-containing Chelators: from Coordination Chemistry to Target-Specific Delivery of Radioactivity

João D. G. Correia, António Paulo and Isabel Santos*

Unidade de Ciências Químicas e Radiofarmacêuticas, Instituto Tecnológico e Nuclear, Estrada Nacional 10, 2686-953 Sacavém, Portugal

*isantos@itn.pt

Review Submitted to Current Radiopharmaceuticals

Keywords: Radiopharmaceuticals; Rhenium; Technetium-99m; Pyrazolyl-containing Ligands; Bifunctional Chelators; Biomolecules.

Abstract

The design of novel target-specific imaging agents based on ^{99m}Tc requires a considerable development of its coordination chemistry. Among all oxidation states available for technetium (-I to VII), the V oxidation state has been the most extensively studied in radiopharmaceutical chemistry, and the majority of the ^{99m}Tc -radiopharmaceuticals in clinical use contain the core $[\text{}^{99m}\text{Tc}(\text{O})]^{3+}$. More recently, the remarkable features of the organometallic precursor $\text{fac-}[\text{M}(\text{CO})_3(\text{H}_2\text{O})_3]^+$ (M = Re, Tc), introduced by Alberto et al., brought renewed interest in the design of innovative low-oxidation ^{99m}Tc -based radiopharmaceuticals. Owing to our interest on the design of innovative target-specific radioactive probes, we have been recently involved in the study of the chemistry of $[\text{M}(\text{O})]^{3+}$ and $\text{fac-}[\text{M}(\text{CO})_3]^+$ (M = Re, Tc) with chelators combining a pyrazolyl unit with aliphatic amines and/or carboxylic acids or thioethers. Such research efforts are reviewed herein, where we present an overview of the chemistry, radiochemistry and biological properties of Re and ^{99m}Tc complexes anchored by those pyrazolyl-containing chelators with relevance in radiopharmaceutical research. The revised work focuses mainly on tricarbonyl M(I) complexes but M(V) oxocomplexes are also covered. This contribution intends to highlight the potential of pyrazolyl-containing chelators for the labeling of biologically active molecules with $^{99m}\text{Tc}(\text{I})$, being presented a variety of examples which include peptides, peptide nucleic acids, inhibitors/substrates of enzymes and DNA-binders.

Contents

1 - Introduction

2 – Neutral and Anionic Pyrazolyl-Containing Chelators

2.1 – $^{99m}\text{Tc}/\text{Re}$ Complexes with the $[\text{M}(\text{O})]^{3+}$ Core

2.2 – $^{99m}\text{Tc}/\text{Re}$ Complexes with the *fac*- $[\text{M}(\text{CO})_3]^+$ Core

2.3 - $^{99m}\text{Tc}/\text{Re}$ Tricarbonyl Complexes Anchored by Bifunctional Chelators

3- Target-Specific Complexes

3.1 – Introduction

3.2 – Peptides

3.3 – Peptide Nucleic Acids

3.4. - Small Biomolecules

3.5 – DNA-Binders

4 – Conclusions

5 – Acknowledgments

6 - References

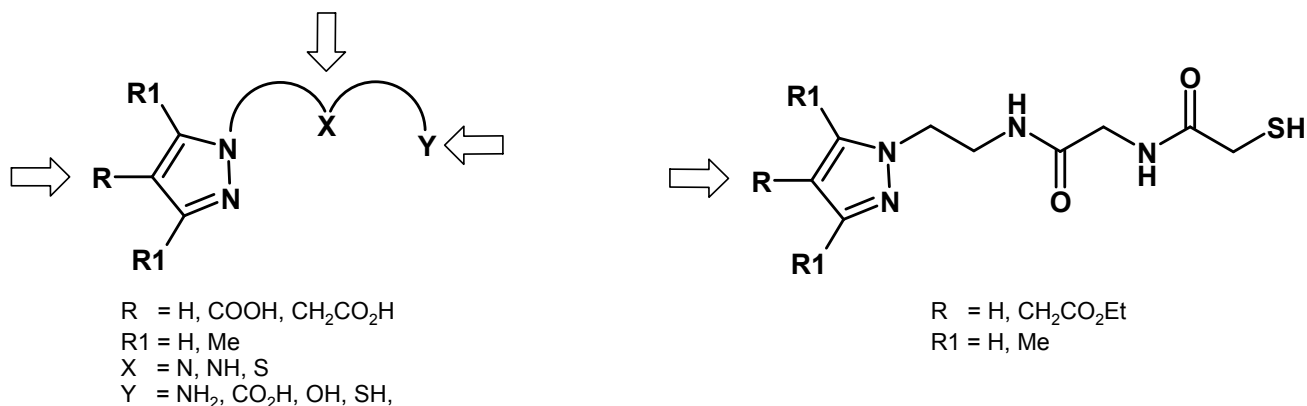
1 – Introduction

Radiopharmaceuticals are drugs having in their composition a radionuclide and are used in nuclear medicine for diagnosis and therapy. The biodistribution of such compounds can be either determined by their chemical and physical properties – *perfusion agents*- or by their biological interactions - *target-specific radiopharmaceuticals* [1]. For the so called *perfusion agents*, the biological distribution is determined by blood flow, and they target high capacity systems, such as phagocytosis, hepatocyte clearance and glomerular filtration. The *target-specific radiopharmaceuticals* target low capacity systems, and their biodistribution is also determined by specific protein interactions, for example enzymatic- or receptor-binding interactions. The radiopharmaceuticals for diagnostic contain gamma- or positron-emitting radionuclides, being suitable for single photon emission tomography (SPECT) or positron emission tomography (PET), respectively [1,2]. The radiotracers in clinical use for diagnostic are predominantly metal-based complexes and the great majority of SPECT diagnostic radiopharmaceuticals currently available in nuclear medicine are either ^{99m}Tc complexes or target-specific biomolecules labeled with ^{99m}Tc or ^{111}In [3]. The preferential use of ^{99m}Tc , considered the workhorse of nuclear medicine, reflects the ideal nuclear properties of this radionuclide ($t_{1/2} = 6.02$ h; $E_{\gamma\text{max}} = 140$ keV), its low-cost and convenient availability from $^{99}\text{Mo}/^{99m}\text{Tc}$ commercial generators. Another relevant feature of ^{99m}Tc relates with its diverse and rich redox chemistry. However, the design of an imaging agent based on a radiometal, namely ^{99m}Tc , requires a considerable development of its coordination chemistry. From all oxidation states available for technetium (from -I to VII), $^{99m}\text{Tc(V)}$ has been the most extensively studied in radiopharmaceutical chemistry, and the cores $[\text{}^{99m}\text{Tc(O)}]^{3+}$, *trans*- $[\text{}^{99m}\text{Tc(O)}_2]^+$, $[\text{}^{99m}\text{Tc(N)}]^{2+}$ and $[\text{}^{99m}\text{Tc-HYNIC}]$ the most exploited [3-9]. In general, low oxidation states have received little attention, despite the noteworthy success of the organometallic complex $[\text{}^{99m}\text{Tc}(\text{CNCH}_2\text{C}(\text{CH}_3)_2\text{OCH}_3)_6]^+$ (Sestamibi), which has been approved a few decades ago as a myocardium imaging agent [1]. Despite its clinical importance, Sestamibi was not a good precursor

to enter into the chemistry of Tc(I) due to its high stability. In this respect, the new organometallic *fac*- $[\text{M}(\text{CO})_3(\text{H}_2\text{O})_3]^+$ (M = Re, Tc), introduced by Alberto et al, is an excellent precursor and has brought renewed interest in the design of radiopharmaceuticals based on low-oxidation states [10-13]. The easy preparation of *fac*- $[\text{M}(\text{CO})_3(\text{H}_2\text{O})_3]^+$ (M=Re, Tc) directly from $[\text{MO}_4]^-$, the chemical robustness of the *fac*- $[\text{M}(\text{CO})_3]^+$ core, and the lability of the three water molecules offered a great number of advantages for the design of innovative radiopharmaceuticals. Moreover, the small size of the *fac*- $[\text{M}(\text{CO})_3]^+$ core is expected to allow the labeling of low molecular weight biomolecules with retention of biological activity and specificity. However, the advances in the development of new Tc(I)-based radioactive probes for *in vivo* targeting of macromolecular structures still depend on the availability of chelating systems well-suited to be combined with different biomolecules [10-13]. In this sense, the chelates should distinguish themselves by high stability, small size, adaptable lipophilicity, absence of isomerism, and easy functionalization. Taking such prerequisites into account, a wide variety of bidentate and tridentate ligands have been evaluated as potential bifunctional chelators for labeling biologically interesting molecules with *fac*- $[\text{}^{99\text{m}}\text{Tc}(\text{CO})_3]$ [10-13].

In the past few years, almost all oxidation states and cores of technetium have been reviewed, showing the role of Tc-coordination chemistry in the development of *target-specific radiopharmaceuticals* [3-13]. In these reviews, aspects such as the importance of the donor atom set on the thermodynamic stability and kinetic inertness of the metal complexes, the use of pharmacokinetic modifying linkers to improve target-to-background ratios and the effect of the bifunctional chelators on the affinity and specificity of the biomolecule for the target have also been discussed.

Owing to our interest on radiopharmaceutical chemistry, namely on the design of innovative target-specific radioactive probes, we have been studying the chemistry of $[\text{M}(\text{O})]^{3+}$ and *fac*- $[\text{M}(\text{CO})_3]^+$ (M = Re, Tc) with different chelators, which combine a pyrazolyl unit with aliphatic amines and/or carboxylic acids, phenols or thioethers, as shown in **Scheme 1**.



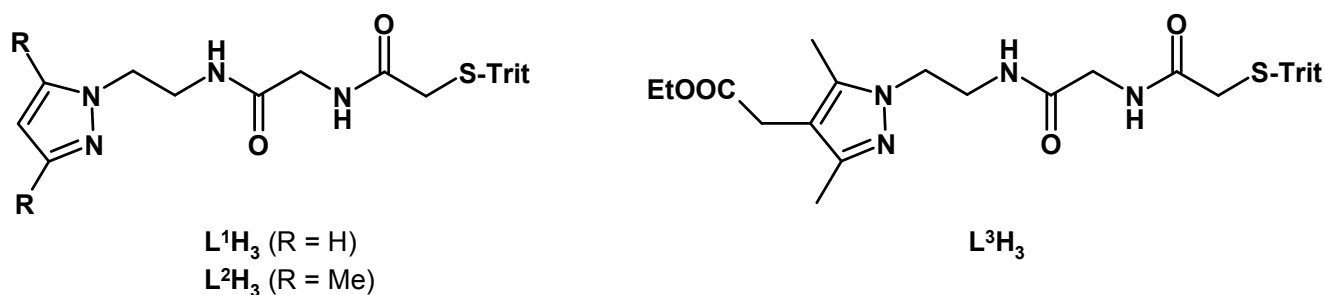
Scheme 1 – Pyrazolyl-based chelators. The potential sites for conjugation of biomolecules are marked.

These pyrazolyl-based chelators present a wide range of adequate features for the development of new target-specific probes, namely high stability, water solubility, different coordination possibilities and easy functionalization. These set of features confer an high degree of versatility to the chelators, making them quite suitable for the stabilization of the units $[\text{M}(\text{O})]^{3+}$ or $fac\text{-}[\text{M}(\text{CO})_3]^+$ ($\text{M} = \text{Re, } ^{99\text{m}}\text{Tc}$), for conjugation to biomolecules of different nature, and for modulation of the pharmacokinetics of the final complexes. Herein, we will highlight relevant aspects of the chemistry of these pyrazolyl-containing chelators with the $[\text{M}(\text{O})]^{3+}$ or $fac\text{-}[\text{M}(\text{CO})_3]^+$ cores, as well as the suitability of the resulting building blocks for labeling biomolecules with $^{99\text{m}}\text{Tc}$. A special effort will be done to correlate the physico-chemical properties of the complexes with their biological properties and potential applications.

2 – Neutral and Anionic Pyrazolyl-Containing Chelators

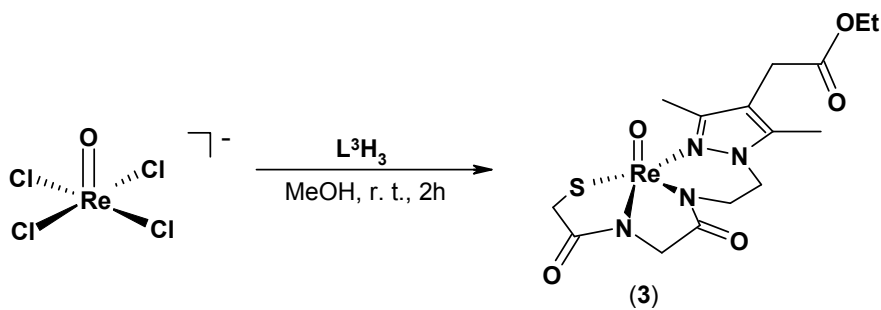
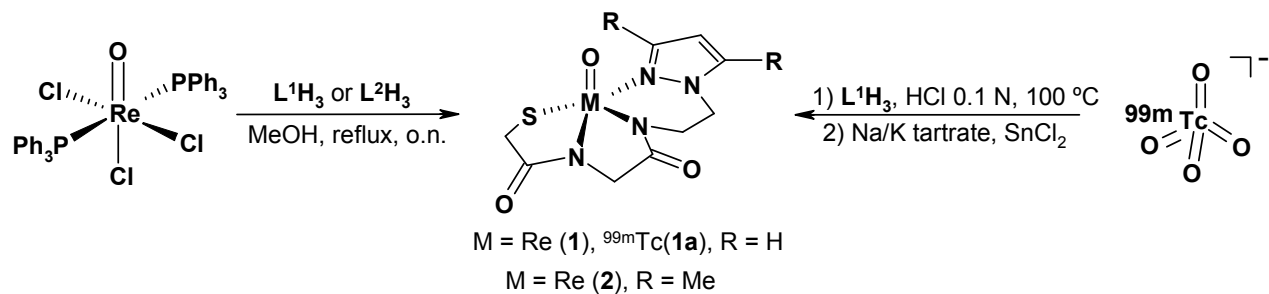
2.1 – $^{99m}\text{Tc}/\text{Re}$ complexes with the $[\text{M}(\text{O})]^{3+}$ Core

The coordination capability of novel tetradentate chelators (L^1H_3) – (L^3H_3) of the N_3S type (**Scheme 2**), obtained by combining a pyrazolyl group with a mercaptoacetylglycine unit, was evaluated towards the $[\text{M}(\text{O})]^{3+}$ ($\text{M} = \text{Re}, ^{99m}\text{Tc}$) cores, aiming to assess their interest as potential bifunctional ligands [14]. It was expected that the aromatic pyrazolyl ring would confer some rigidity to the complexes with the consequent enhancement of their stability. The presence of a carboxylic acid group in the aromatic pyrazolyl ring in L^3H_3 should allow an easy coupling of biologically relevant molecules to the metal center.



Scheme 2 - Tetradentate pyrazolyl-based N_3S -donor chelators

Reaction of adequate $\text{Re}(\text{V})$ starting materials with the trityl-protected chelators L^1H_3 – L^3H_3 afforded almost quantitatively the neutral complexes $[\text{ReO}(\text{L})]$ ($\text{L} = \text{L}^1$ (**1**); L^2 (**2**); L^3 , (**3**)) (**Scheme 3**). The coordination mode of the chelators was confirmed by NMR studies, including two-dimensional techniques ($^1\text{H}/^1\text{H}$ COSY and $^1\text{H}/^{13}\text{C}$ HSQC), and by X-ray diffraction analysis in the case of (**2**) (Fig. (**1**)). The metal center is five-coordinated, displaying a square pyramidal coordination geometry, as shown in Fig. (**1**).



Scheme 3 – Synthesis of M(V) (M = Re, $^{99\text{m}}\text{Tc}$) oxocomplexes with tetradentate pyrazolyl-based N_3S -donor chelators.

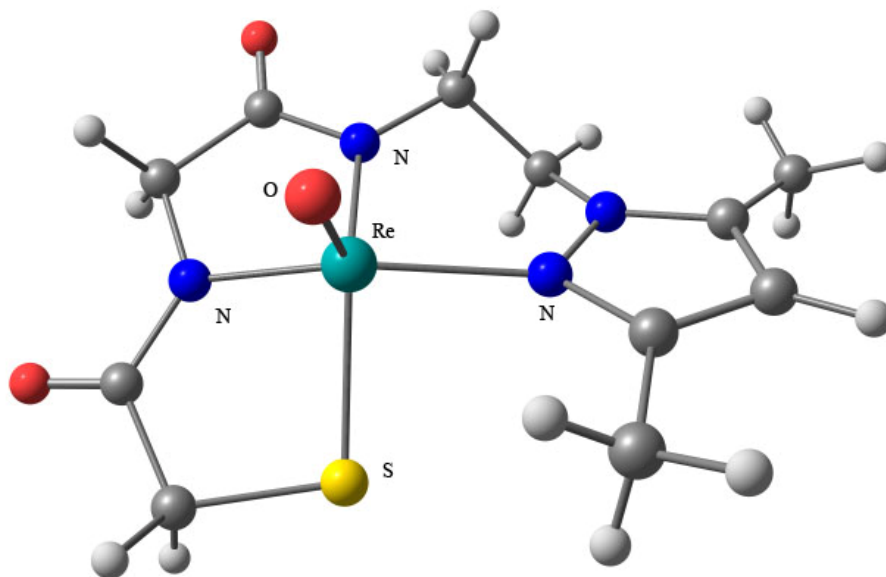
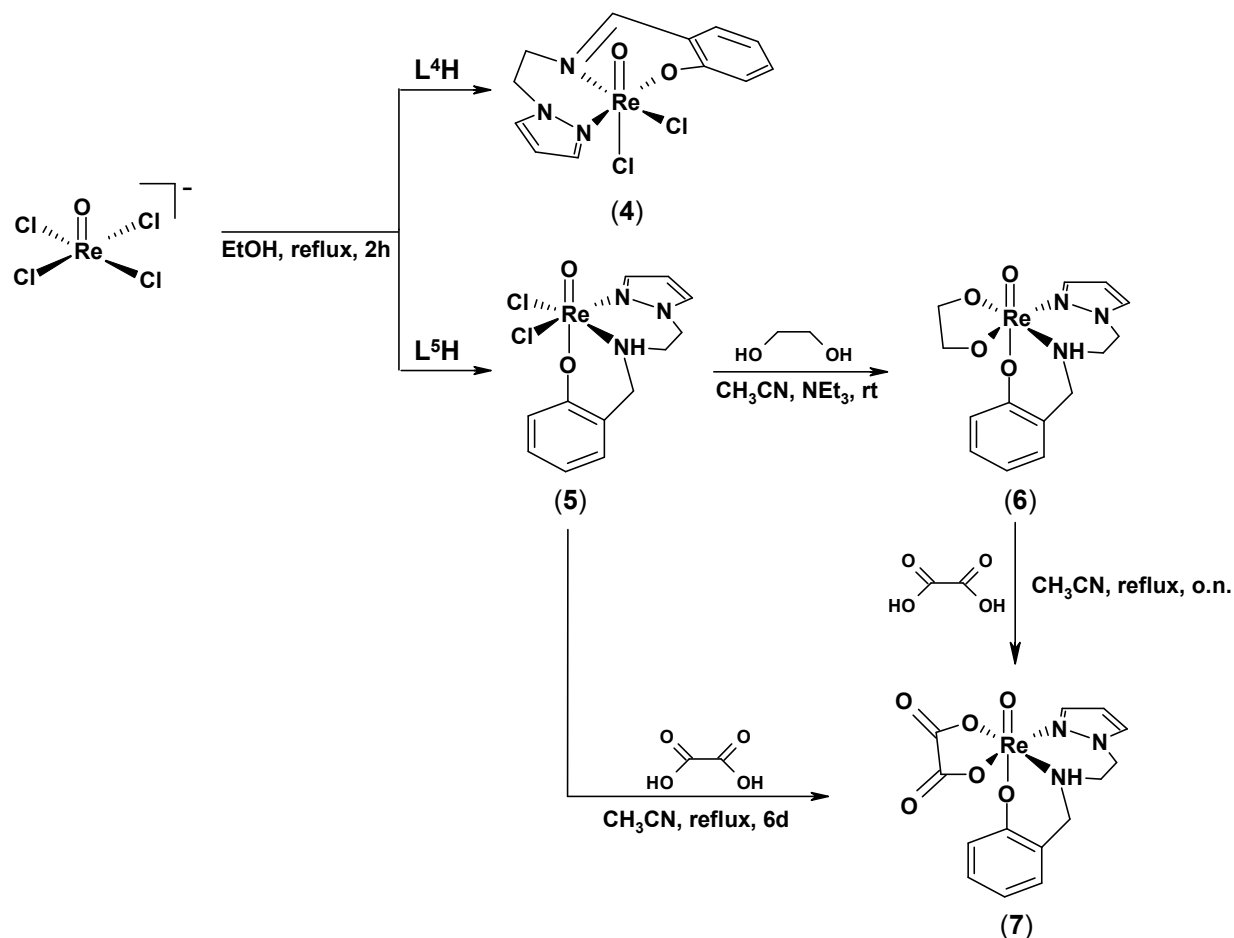


Fig. (1) – Molecular structure of the oxorhenium(V) complex (2) [14].

The synthesis of the congener $[\text{}^{99\text{m}}\text{TcO}(\text{L}^1)]$ (**1a**) was achieved directly from $[\text{}^{99\text{m}}\text{TcO}_4]^-$ in aqueous medium, in almost quantitative yield and with high specific activity and radiochemical purity (**Scheme 3**) [14]. Complex (**1a**) is moderately lipophilic ($\log P_{\text{o/w}} = + 0.73 \pm 0.03$), and displays a high *in vitro* stability in the presence of excess glutathione (10 – 20 mM). Biodistribution studies in mice have shown that (**1a**) undergoes rather slow blood clearance (3.5 ± 0.8 % ID/g blood at 4 h p.i.) being excreted mainly through the hepatobiliary pathway with a relatively low excretion rate (22.6 ± 7.0 % ID at 4 h p.i.). HPLC analysis of the blood and urine of mice injected with (**1a**) has shown that the intact complex is the unique radioactive species detected in the blood but revealed the presence of several metabolites in the urine. These biological data brought together pointed out that tetradentate chelators of the N_3S type containing a pyrazolyl coordinating group are not very promising compounds to be explored as bifunctional ligands for the labeling of biomolecules using $^{99\text{m}}\text{Tc}(\text{V})$ oxocomplexes.

Mixed-ligand $\text{M}(\text{V})$ oxocomplexes of the so called “3+1” type, bearing tridentate/dinegative ligands and unidentate thiolate co-ligands, have been largely explored for labeling biomolecules, in alternative to the more classical approach based on oxocomplexes anchored by tetradentate chelators [4,5]. However, with a few exceptions, these mixed-ligand complexes showed a pronounced tendency to undergo *trans*-chelation reactions *in vivo* as a result of available vacant coordination sites [4,5]. To circumvent this problem, several authors have focused on closed shell and hexa-coordinated “3+2” $\text{M}(\text{V})$ oxocomplexes. Most of the reported $\text{Re}(\text{V})/\text{Tc}(\text{V})$ “3+2” oxocomplexes were obtained using a combination of tridentate/dinegative and bidentate/uninegative ligands containing *P*, *N*, *S* or *O* donor atoms. “3+2” Oxocomplexes anchored by tridentate/uninegative and bidentate/dinegative chelators are more scarce, being limited to a few examples of $\text{Re}(\text{V})$ compounds [4]. The suitability of the potentially tridentate/uninegative pyrazolyl-containing chelators 2-[2-(pyrazol-1-yl)ethyliminomethyl]phenol (**L⁴H**) and 2-[2-(pyrazol-1-yl)ethylaminomethyl]phenol (**L⁵H**) to stabilize “3+2” mixed-ligand complexes was evaluated, using the corresponding oxo-dichlorides as starting

materials and different bidentate co-ligands [15]. The compounds *mer*-[ReO(L⁴)Cl₂] (**4**) and *fac*-[ReO(L⁵)Cl₂] (**5**) were synthesized by reaction of the precursor (NBu₄)[ReOCl₄] with L⁴H and L⁵H, as shown in **Scheme 4**.



Scheme 4 – Oxorhenium(V) complexes (**4**) – (**7**) anchored by a pyrazole-containing Schiff base (L⁴) and respective amine (L⁵).

The reactivity of (**5**) towards potential bidentate/dianionic substrates has shown that the type of reaction observed is strongly dependent on the donor atom set of the incoming ligand. The presence of sulphur favors the displacement of the ancillary ligand (L⁵), preventing the formation of mixed-ligand complexes. By contrast, complex (**5**) reacted with (O,O)-bidentate substrates (1,2-ethanediol and oxalic

acid) providing the air and water-stable *fac*-[ReO(L⁵)(OCH₂CH₂O)] (**6**) and *fac*-[ReO(L⁵)(C₂O₄)] (**7**). These complexes have been characterized by the common spectroscopic techniques (IR, ¹H and ¹³C NMR), and also by X-ray diffraction analysis (Fig. (2)). In these complexes the metal is six-coordinated by the oxo-group and by the tridentate and bidentate chelators, displaying an octahedral coordination geometry, as depicted Fig. (2). These new (N,N,O)/(O,O) mixed-ligand oxorhenium(V) complexes did not emerge as promising tools to be further explored in radiopharmaceutical research due to the marked tendency of the respective ancillary ligand (L⁵) to be replaced by thiol groups, which are ubiquitous in biological substrates like glutathione.

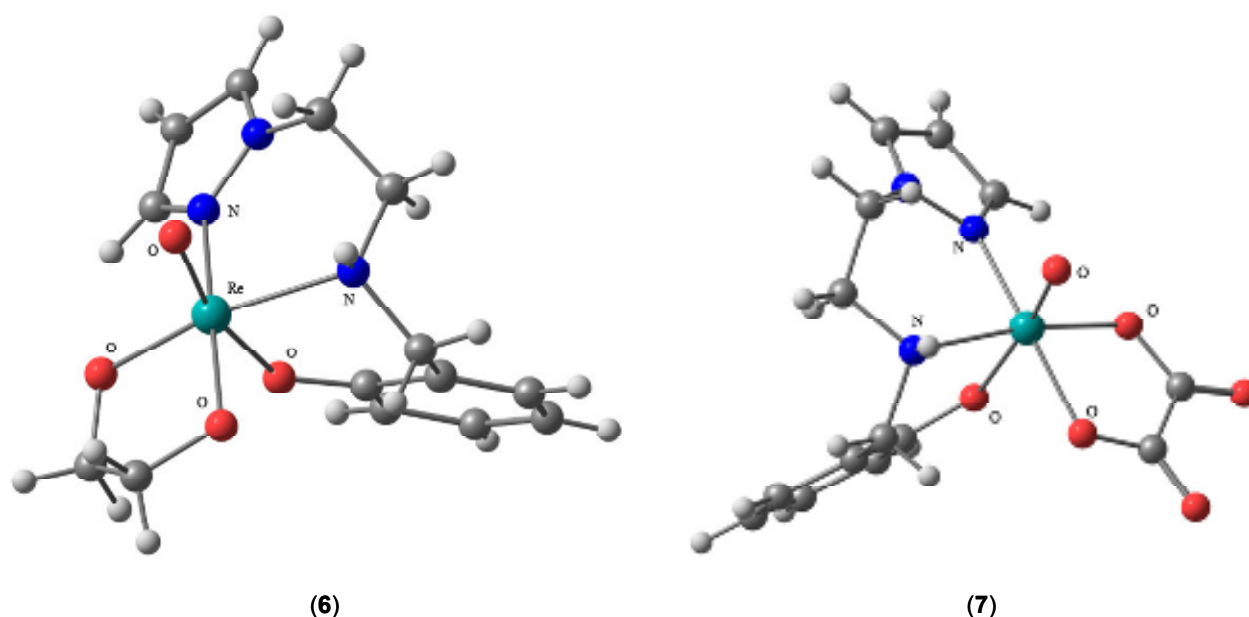
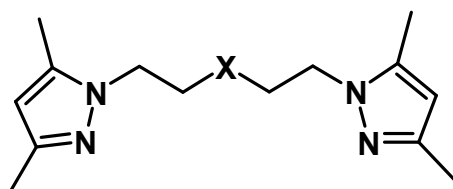


Fig. (2) – Molecular structures of the oxorhenium(V) complexes (**6**) and (**7**) [15].

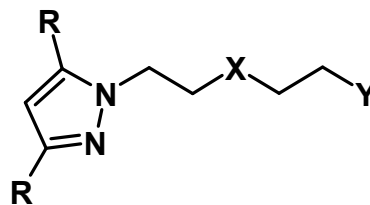
2.2 – ^{99m}Tc/Re Complexes with the *fac*-[M(CO)₃]⁺ Core

To access a general labeling protocol for biomolecules with ^{99m}Tc(I), we have been exploring the pyrazolyl-containing compounds displayed in **Scheme 5** [16-19].



X = NH, (**L**⁶)

X = S, (**L**⁷)



R = Me:

X = NH, Y = NH₂, (**L**⁸)

X = S, Y = NH₂, (**L**⁹)

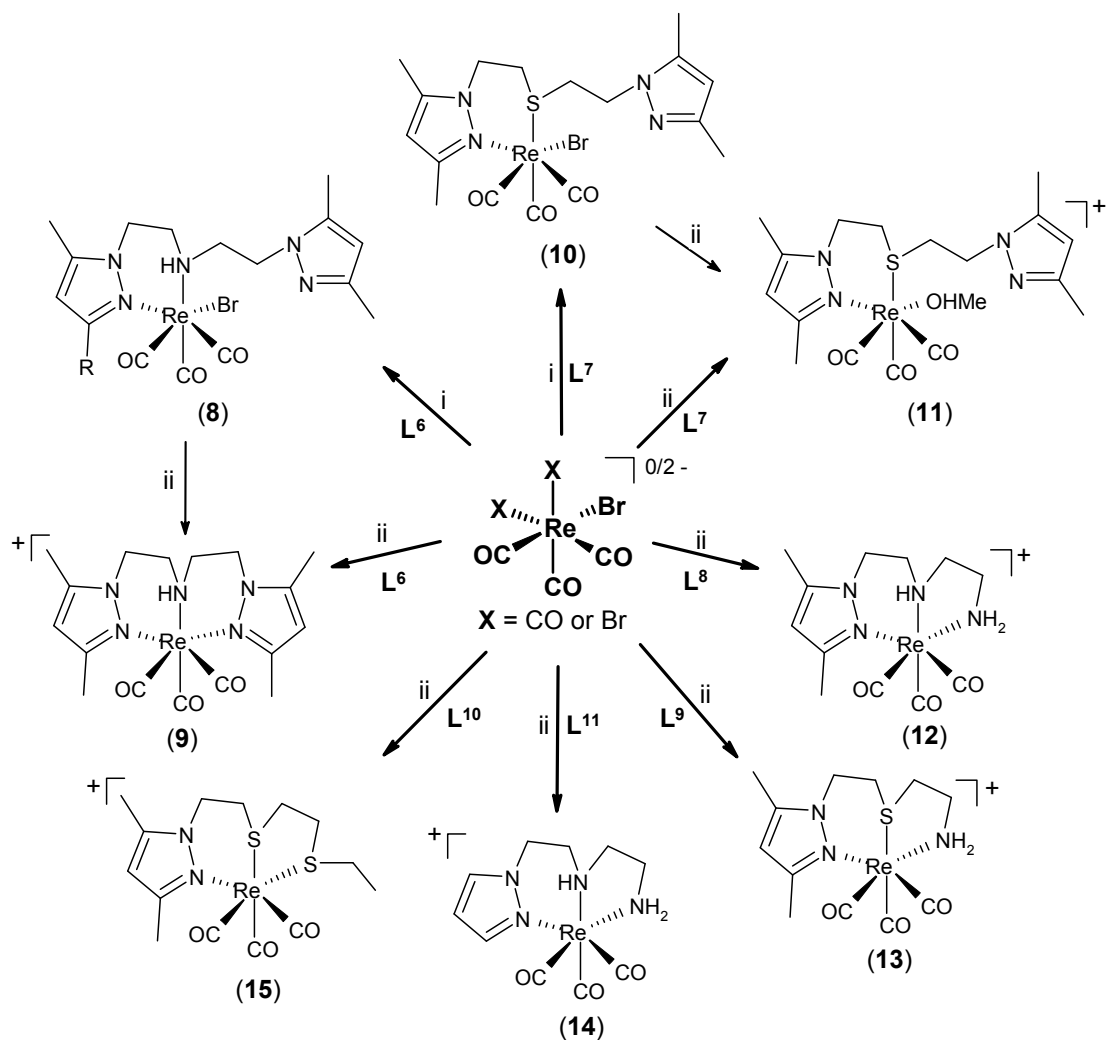
X = S, Y = SCH₂CH₃, (**L**¹⁰)

R = H:

X = NH, Y = NH₂, (**L**¹¹)

Scheme 5 – Pyrazolyl-containing ligands (**L**⁶) - (**L**¹¹).

The ligands (**L**⁶) – (**L**¹¹) stabilize the *fac*-[Re(CO)₃]⁺ moiety forming the well defined complexes (**8**) – (**15**) with a metal-to-ligand ratio 1:1 (**Scheme 6**).



Scheme 6 –Synthesis of the Re(I) complexes (8) – (15): i) MeOH, rt; ii) MeOH, reflux.

The asymmetric ligands always coordinate as tridentate ((12) – (15)), while the coordination behavior of the symmetric ones, (L^6) and (L^7), depends on the nature of the donor atom set. Higher temperature forces the tridentate coordination of (L^6) through the three nitrogen atoms (9), while in the case of (L^7), the presence of the sulfur atom prevents the coordination of the second pyrazolyl ring (11). The coordination mode of this family of chelators was established by X-ray structural analysis (Fig. (3)) and by NMR spectroscopy.

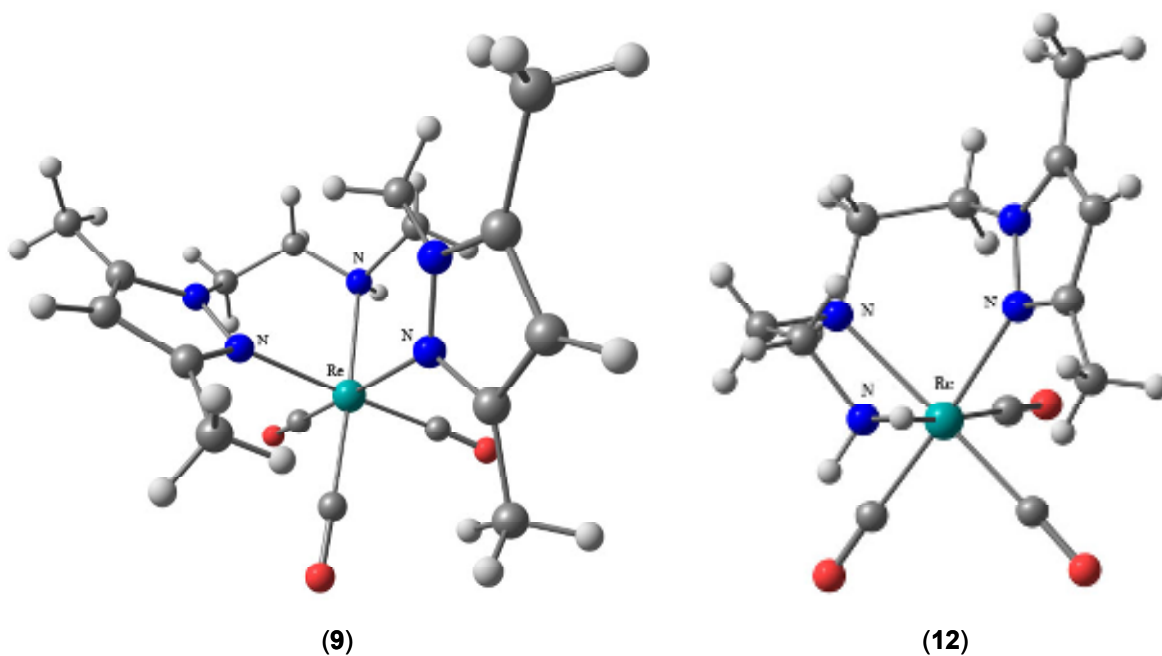
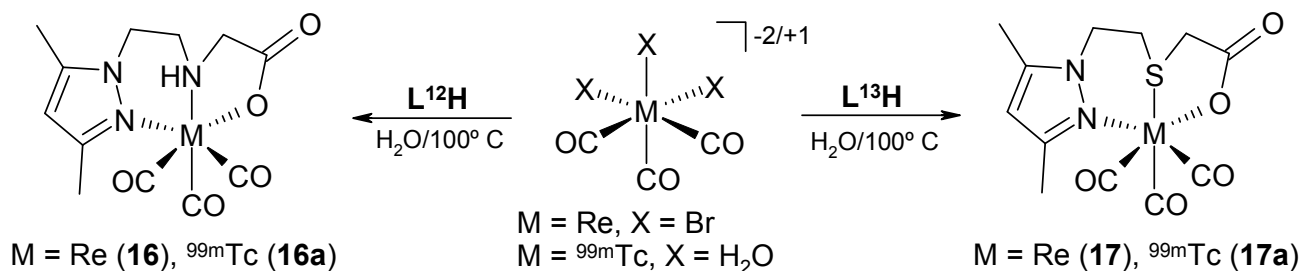


Fig. (3) – Molecular structures of the tricarbonyl rhenium complexes **(9)** and **(12)** [16].

Reaction of the chelators (**L⁶**) and (**L⁸**) – (**L¹¹**) with the organometallic precursor *fac*- $[\text{}^{99\text{m}}\text{Tc}(\text{CO})_3(\text{H}_2\text{O})_3]^+$ allowed the preparation of the analog cationic $^{99\text{m}}\text{Tc}(\text{I})$ complexes (**9a**) and (**12a**) – (**15a**) in high yield and high radiochemical purity [17-19]. The *in vitro* studies performed revealed that the pyrazole-diamine-containing complexes, (**12a**) and (**14a**), were prepared with higher specific activity, being more resistant to *in vitro* challenge with biologically relevant amino acid substrates like histidine or cysteine, when compared with the related cations anchored by pyrazole-dithioether chelators (N,S,S-donors). Biodistribution studies in mice indicated also that the complexes stabilized by ligands containing the pyrazolyl-diamine backbone are highly stable *in vivo*, presenting a fast rate of blood clearance and high rate of total radioactivity excretion, occurring primarily through the renal-urinary pathway.

We have also introduced and studied the novel potentially monoanionic chelators (**L^{12H}**) (N,N,O - donor atom set) and (**L^{13H}**) (N,S,O - donor atom set), which form neutral complexes of the type *fac*-

$[M(\text{CO})_3(\text{k}^3\text{-L})]$ ($M = \text{Re}, {}^{99\text{m}}\text{Tc}$; $L = (\mathbf{L}^{12}), (\mathbf{L}^{13})$) by reaction with the appropriate precursor, under optimized reaction conditions (**Scheme 7**) [20,21].



Scheme 7 –Synthesis of $\text{Re}/{}^{99\text{m}}\text{Tc}$ complexes of the type *fac*- $[\text{M}(\text{CO})_3(\text{k}^3\text{-L})]$ stabilized by anionic pyrazolyl-based chelators with N,X,O ($X = \text{N}, (\mathbf{L}^{12}); \text{S}, (\mathbf{L}^{13})$) donor atom sets.

Complexes (**16**) and (**17**) have been fully characterized by the usual analytical techniques, including by X-ray crystallography. The complexes are neutral, and the metal is six-coordinated by three carbonyl ligands and by the monoanionic chelators, which act as tridentate through N,N,O (**16**) and N,S,O (**17**) donor atom sets as displayed in Fig. (4).

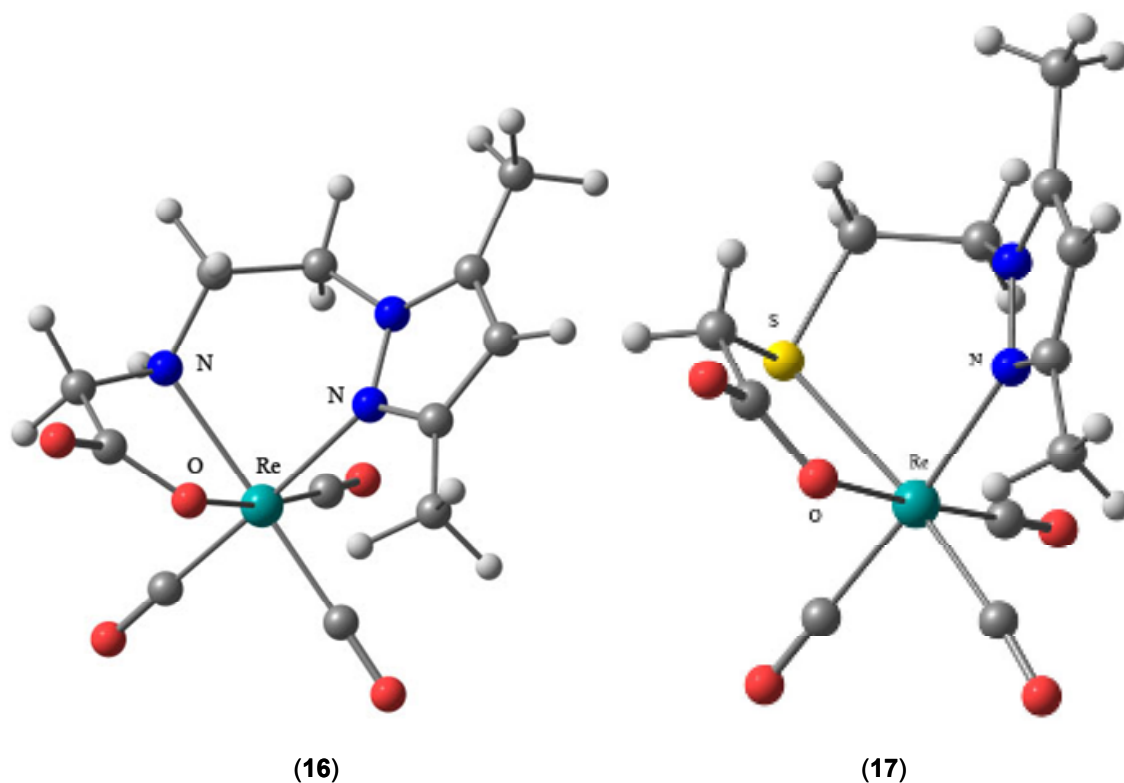


Fig. (4) – Molecular structures of the tricarbonyl rhenium complexes **(16)** and **(17)** [20,21].

The NNO-donor (**L¹²**) appeared as the most promising monoanionic chelator to be further explored in the design of bifunctional chelating ligands for the labeling of small biomolecules, mainly due to the enhanced *in vitro* stability and more favourable biological profile of the corresponding ^{99m}Tc(I) complex **(16a)**.

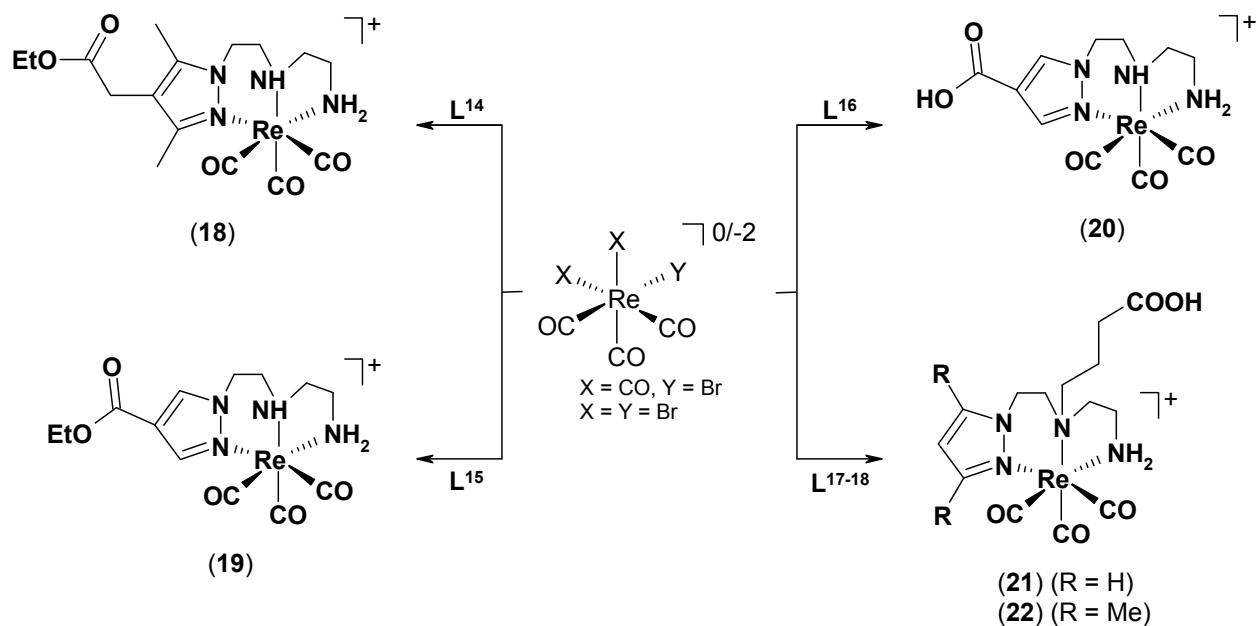
All together, the *in vitro* and *in vivo* evaluation of ^{99m}Tc(I) tricarbonyl complexes anchored by neutral (**Scheme 6**) or monoanionic pyrazolyl-containing chelators (**Scheme 7**) has shown that the replacement of amines by thioether coordinating groups led to complexes with lower specific activity, and less resistant to *in vitro* challenge with biologically relevant substrates, like histidine and cysteine. DFT (density functional theory) calculations have been performed in order to have a more rationale insight into the influence of the ligand donor atom set (N,N,O vs N,O,S; N,N,N vs N,N,S vs N,S,S) on the *in vitro* stability of neutral and cationic ^{99m}Tc(I) complexes with tridentate pyrazolyl-containing ligands [21]. These studies have shown that the replacement of nitrogen by sulfur donor atoms led to slightly

less stable complexes ($\Delta E \sim 4\text{-}10$ kcal/mol). However, these differences are not significant enough to explain the lower *in vitro* stability observed experimentally for the complexes with the ligands containing sulfur donor atoms, suggesting that such trend is not explained by thermodynamic factors and relies most likely on kinetic effects [21].

2.3 - $^{99m}\text{Tc/Re}$ Tricarbonyl Complexes Anchored by Bifunctional Chelators

Owing to their highest specific activity, highest *in vitro/in vivo* stability and more favourable pharmacokinetics, the Tc(I) complexes anchored by asymmetric pyrazolyl-diamine ligands (N,N,N-donors) and pyrazolyl-aminocarboxylic acid ligands (N,N,O-donors) have emerged as the best suited for the design of targeted-specific radiopharmaceuticals. An intrinsic advantage of these systems is their chemical versatility, which allows an easy control of the size and lipophilicity of the complexes, by varying the substituents at the aromatic ring, and different possibilities for biomolecules coupling, with retention of the coordination sphere. Such coupling can be done either at the pyrazolyl ring or at an aliphatic side chain attached to the ligand, through the use of an appropriate functional group (e.g. carboxylic acid).

Novel bifunctional chelating ligands, (\mathbf{L}^{14}) – (\mathbf{L}^{18}), analogs of the lead compounds (\mathbf{L}^8) and (\mathbf{L}^{11}), have been prepared using a multistep approach [18,19,22]. These chelators combine a N,N,N donor atom set for metal coordination and carboxylate pendant arms in the aromatic ring ((\mathbf{L}^{14}) – (\mathbf{L}^{16})) or at the central amine of the ligand backbone ((\mathbf{L}^{17}) and (\mathbf{L}^{18})) for coupling to biomolecules. The bifunctional chelators (\mathbf{L}^{14}) – (\mathbf{L}^{18}) reacted with adequate precursors to afford complexes of the type *fac*- $[\text{Re}(\text{CO})_3(\text{k}^3\text{-L})]$ ($\text{L} = (\mathbf{L}^{14}) - (\mathbf{L}^{18})$, **Scheme 8**), in which the chelators act as tridentate through the nitrogen atoms, similarly to what has been observed with the corresponding model complexes (**12**) and (**14**) (**Scheme 6**).



Scheme 8 - Synthesis of the tricarbonyl rhenium complexes **(18)** – **(22)**.

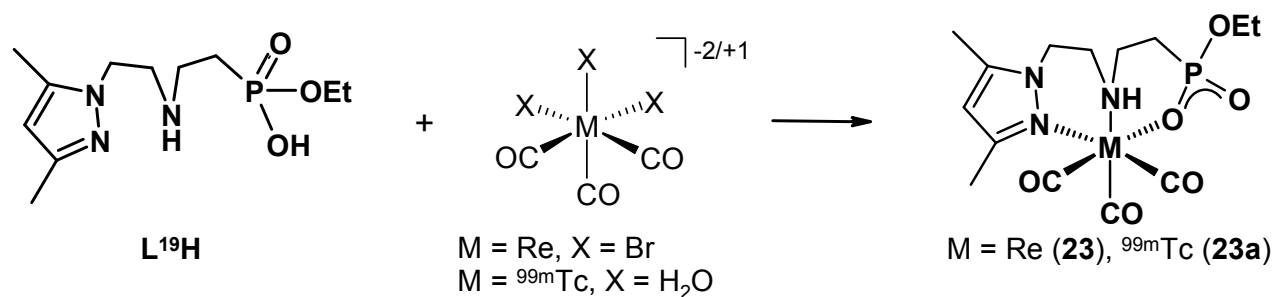
The $^{99\text{m}}\text{Tc}$ analogs **(18a)** – **(22a)** were obtained in high yields ($\geq 90\%$) with high radiochemical purity and specific activity, using ligand concentrations spanning from 10^{-4} to 10^{-5} M. All complexes are generically stable *in vitro*, namely against cysteine and histidine exchange reactions.

The biological properties of the cationic complexes **(20a)** and **(22a)** were assessed in CD1 mice at different time points, and compared with the pharmacokinetic profile of the analog model radioactive complexes **(14a)** and **(12a)**, respectively [19, 23]. The resulting data showed that all complexes were rapidly cleared from blood and other main organs, primarily through the renal-urinary pathway with a small portion retained in the hepatobiliary tract. The main differences in the biodistribution of the different complexes were related to the clearance from tissues as well as to the rate of overall excretion. The compounds containing pendant free carboxylic acid groups **(20a)** and **(22a)** showed a faster clearance from the main organs and the total radioactivity excretion was relatively enhanced while the hepatic retention was reduced, as compared to the model complexes **(14a)** and **(12a)**. This trend is however more pronounced in the case of **(20a)**. As expected, the hepatic retention of the complexes is

also related with their lipo(hydro)philic character. In fact, **(20a)**, which is the complex with the lowest hepatic retention, is also the less lipophilic ($\log P_{o/w} = -2.35 \pm 0.01$) compared to the model complex **(14a)** ($\log P_{o/w} = -0.93 \pm 0.01$).

In conclusion, the general features of the $^{99m}\text{Tc(I)}$ complexes containing the bifunctional chelating ligands (**L¹⁶**) and (**L¹⁸**), such as *in vitro* stability, lipophilicity, and biological profile are very promising for labeling biologically active compounds.

Aiming to develop new strategies for the labeling of hydroxyl-containing biomolecules with the organometallic core $\text{fac-}[^{99m}\text{Tc}(\text{CO})_3]^+$, we have also introduced a new chelator containing a pyrazolyl-amine backbone and a phosphonate monoester (**L^{19H}**) [24], which upon reaction with the corresponding organometallic precursor afforded the complexes $\text{fac-}[\text{M}(\text{CO})_3(\text{k}^3\text{-L}^{19})]$ ($\text{M} = \text{Re}$, **(23)**; ^{99m}Tc , **(23a)**) (Scheme 9). The radiocomplex is stable both *in vitro* and *in vivo*, without any measurable decomposition or reoxidation. Biodistribution studies of **(23a)** in mice indicated a rapid blood clearance, as well as a relatively fast clearance from main organs, being excreted mainly through the hepatobiliary pathway.

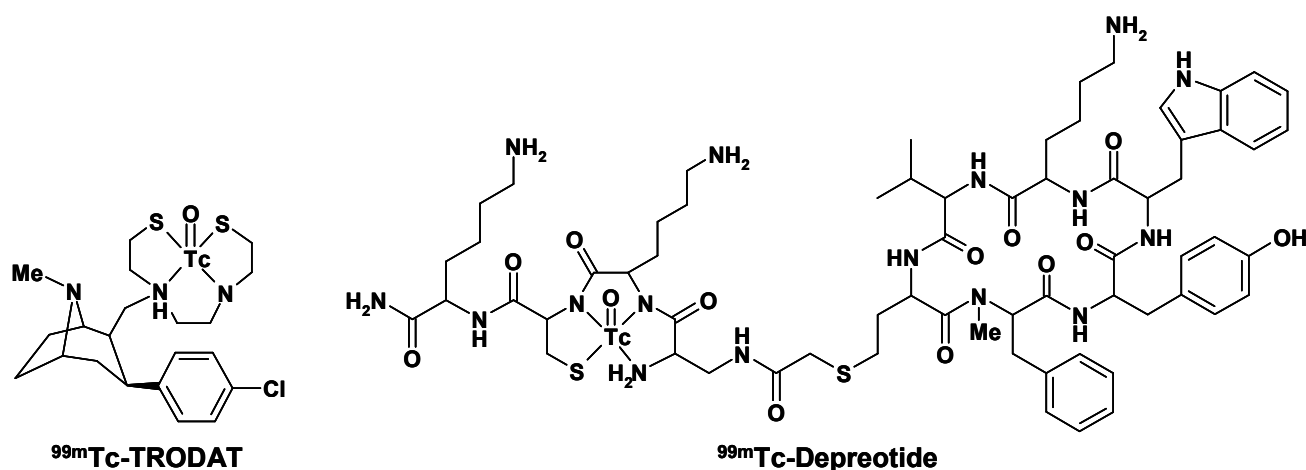


Scheme 9 – Preparation of the tricarbonyl complexes **(23)** and **(23a)**.

3- Target-Specific Complexes

3.1 Introduction

A great variety of biologically relevant molecules (“biomolecules”) based on monoclonal antibodies, peptides, non-peptidic small molecules, and oligonucleotide analogs, have been explored for target-specific delivery of radionuclides [3, 25-31]. These biomolecules must recognize cell surface markers or receptors over-expressed on malignant cells, intracellular metabolic pathways that are up-regulated in cancer, endogenous analogs utilization or cellular processes closer to transcription. So far, among all the possible approaches for the design of target-specific radiopharmaceuticals, the use of bifunctional chelators for linking the radionuclide to the biomolecules has been the most successful. In the case of ^{99m}Tc , we may refer [$^{99m}\text{Tc}(\text{O})(\text{TRODAT})$] and ^{99m}Tc -depreotide (NeoTect[®]) as successful examples of such approach (Scheme 10) [1, 3, 32]. [$^{99m}\text{Tc}(\text{O})(\text{TRODAT})$] has been developed for imaging the dopamine transporter (DAT) for diagnosis of Parkinson’s disease, while ^{99m}Tc -depreotide is a peptide-based compound for imaging somatostatin receptor-positive tumors in lungs.



Scheme 10 – Target-specific radiopharmaceuticals.

Taking into account the clinical relevance of different receptor families, intracellular metabolic pathways or endogenous gene expression, we have investigated the possibility of using bioactive

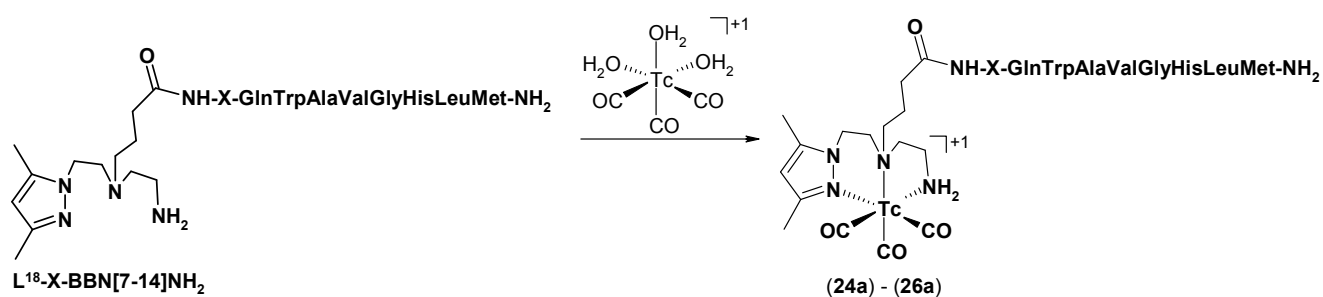
peptides, oligonucleotide analogs or low molecular weight compounds such as enzyme inhibitors/substrates (tyrosine kinase and inducible nitric oxide synthase) for target-specific delivery of *fac*-[^{99m}Tc(CO)₃]⁺ [25-31]. To achieve this goal we have explored the bifunctional chelator approach using mainly **L¹⁸** (**Scheme 8**). Recently, we have also studied the conjugation of DNA-binding molecules to some of the above described pyrazolyl-diamine chelators, aiming to explore the possibility of using ^{99m}Tc for targeted therapy.

In the next sections, which are organized according to the nature of the targeting biomolecules, we will present our most relevant achievements in the target-specific delivery of ^{99m}Tc(I)

3.2 – Peptides

During the last decade, a significant research effort has been devoted to the finding of radiolabeled peptides suitable for the *in vivo* detection, functional characterization or therapy of tumors [29-31]. Such research effort has been driven by the favorable features of peptides as carrier molecules that can recognize receptors overexpressed in tumor cells and involved in the different processes that underly tumor pathology, such as proliferation, angiogenesis or metastasis. So far, the most important achievements in this area have been obtained for somatostatin analogs (e.g. ¹¹¹In-DTPA-octreotide - Octreoscan[®]), which are clinically relevant for the management of relatively rare neuroendocrine malignancies [1,29]. At a pre-clinical stage, some progresses have also been reported for other classes of radiolabeled peptides, namely for analogs of bombesin (BBN) or α -melanocyte stimulating hormone (α -MSH), and for peptides containing the Arg-Gly-Asp amino acid sequence (RGD). However, further improvements are still needed for introducing this type of radiolabeled peptides into the clinical practice [30,31]. Aiming to contribute for the accomplishment of such general goal, we have explored the tricarbonyl technology and pyrazolyl-diamine chelators for ^{99m}Tc-labelling of BBN analogs, α -MSH analogs and cyclic RGD-based peptides, as reviewed herein.

Bombesin (BBN) is a 14 amino acid peptide with very high affinity for the gastrin-releasing peptide receptor (GRPr; BB2 or BBN receptor subtype 2). The GRPr is expressed on a variety of tumors including breast, prostate, pancreatic, and small-cell lung cancer [33-36]. Therefore, BBN or BBN derivatives have been utilized as targeting vectors for the design and development of GRPr-specific diagnostic or therapeutic radiopharmaceuticals [37-41]. Pyrazolyl-diamine BBN conjugates of the general structure $L^{18}\text{-X-BBN}[7-14]\text{NH}_2$ ($X = \text{GGG}, \text{SSS}, \beta\text{-alanine}$), which present three different types of linkers between the peptide and the chelator, have been synthesized [19,42]. These conjugates allowed the preparation of the bioactive complexes $[\text{}^{99\text{m}}\text{Tc}(\text{CO})_3(\text{L}^{18}\text{-X-BBN}[7-14]\text{NH}_2)]^+$ ($X = \text{GlyGlyGly}$, (**24a**); SerSerSer, (**25a**); β -alanine, (**26a**)) in high radiochemical yield ($\geq 95\%$) by reaction with the precursor $[\text{}^{99\text{m}}\text{Tc}(\text{CO})_3(\text{H}_2\text{O})]^+$ (**Scheme 11**). All radioactive complexes showed remarkable *in vitro* stability, as monitored by HPLC [19,42].



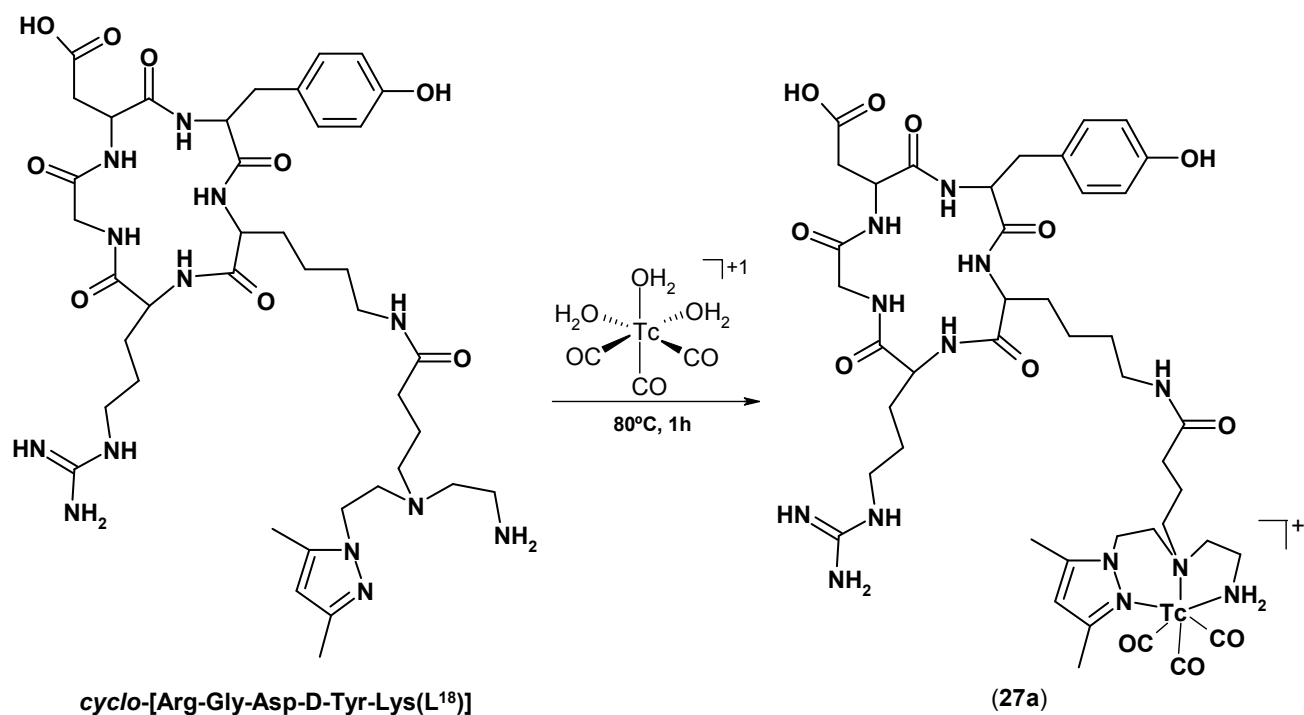
Scheme 11 – Radiosynthesis of the bioactive complexes $[\text{}^{99\text{m}}\text{Tc}(\text{CO})_3(\text{L}^{18}\text{-X-BBN}[7-14]\text{NH}_2)]^+$ ($X = \text{GlyGlyGly}$, (**24a**); SerSerSer, (**25a**); β -alanine (**26a**)).

Competitive binding displacement assays in human prostate PC-3 tumor cells demonstrated specific binding affinity of the $L^{18}\text{-X-BBN}[7-14]\text{NH}_2$ conjugates for the GRPr, with IC_{50} values of 0.2 ± 0.02 nM ($X = \text{GlyGlyGly}$), 1.9 ± 0.10 nM ($X = \text{SerSerSer}$) and 0.7 ± 0.04 nM ($X = \beta\text{-alanine}$). *In vitro* internalization and efflux studies in human prostate PC-3 cells showed an agonistic binding behavior

for the radioconjugates (**24a**) - (**26a**). The highest uptake and residualization of radioactivity was observed for X = β -alanine, (**26a**), however, the exact mechanism for its increased retention is still unclear.

The pharmacokinetic profile and degree of tumor uptake for (**24a**) - (**26a**) was evaluated in SCID mice bearing xenografted human prostate PC-3 tumors. The radiopeptides showed an accumulation in tumor tissues of $1.76 \pm 1.20\%$ (**24a**) ID/g, $1.76 \pm 0.79\%$ ID/g (**25a**), and $1.08 \pm 0.41\%$ ID/g (**26a**) at 1 h pi. Blocking studies with “cold” BBN[1–14] reduced the accumulation of radioactivity in those tissues (~22 – 40% reduction, 1 h pi), demonstrating *in vivo* specificity of these analogues for GRPr-expressing cells.

Radiolabeled peptides containing the Arg-Gly-Asp amino acid consensus sequence (RGD) have also been extensively studied to develop site-directed targeting vectors for integrin receptors upregulated on tumor cells and neovasculature [43-46]. Integrin recognition of the canonical RGD sequence plays a pivotal role in many cell-cell and cell-extracellular matrix (ECM) interactions. The integrins of most interest in cancer imaging and therapy contain the α_v subunit, particularly the $\alpha_v\beta_3$ and $\alpha_v\beta_5$ subtypes [47-49]. Aimed at introducing novel nuclear tools suitable to image angiogenesis and tumor formation *in vivo*, the cyclic RGD-based peptide conjugate *cyclo*-[Arg-Gly-Asp-D-Tyr-Lys(L¹⁸)] has been prepared. This conjugate reacted with $[^{99m}\text{Tc}(\text{CO})_3(\text{H}_2\text{O})]^+$, giving $[^{99m}\text{Tc}(\text{CO})_3\textit{cyclo}$ -[Arg-Gly-Asp-D-Tyr-Lys(L¹⁸)]]⁺ (**27a**) in high yield ($\geq 90\%$) and high specific activity (ca. 6×10^6 Ci/mol) (Scheme (12)) [50].



Scheme 12 – Radiosynthesis of $[\text{}^{99\text{m}}\text{Tc(CO)}_3\text{cyclo-[Arg-Gly-Asp-D-Tyr-Lys(L}^{18}\text{)]}]^+$ (**27a**).

In vitro internalization and blocking assays in $\alpha_v\beta_3$ receptor-positive human M21 melanoma cancer cells showed that the radiopeptide (**27a**) has the ability to target the integrin receptor, with high specificity and selectivity. *In vivo* accumulation of radioactivity in mice bearing either $\alpha_v\beta_3$ receptor-positive or negative human melanoma tumors showed receptor specific uptake of the radiotracer with accumulations of 2.50 ± 0.29 ID/g and $0.71 \pm 0.08\%$ ID/g in $\alpha_v\beta_3$ integrin positive (M21) and negative (M21L) tumors at 1 h post-injection, respectively [50]. A comparative study with other *cyclo*-RGD peptides labeled with different $^{99\text{m}}\text{Tc}$ -cores revealed that (**27a**) competed well with the best performing compound ($[\text{}^{99\text{m}}\text{Tc}]\text{EDDA/HYNIC-RGD}$) in terms of pharmacokinetic profile and receptor-mediated tumor uptake in mice bearing either $\alpha_v\beta_3$ receptor-positive or negative human melanoma tumors [51].

Most murine and human melanoma metastasis bear upregulated α -melanocyte stimulating hormone (α -MSH) receptors, namely the melanocortin type 1 receptor (MC1R). α -MSH is the most potent naturally

occurring melanotropic peptide and the most active peptide of MC1R (Table 1) [52-54]. Therefore, in the last few years, a great deal of effort has been directed towards the development of radiolabeled analogs of the tridecapeptide α -MSH for diagnosis and treatment of melanoma [55-61]. Aiming to target the MC1R *in vivo*, we focused our attention on the labeling of α -MSH analogs containing the bifunctional chelator L^{18} (Table 1, entries 3, 4 and 6) with the moiety *fac*- $[^{99m}\text{Tc}(\text{CO})_3]^+$ [62-64].

Table 1 – Structure of α -melanocyte-stimulating hormone and analogues

Entry	PEPTIDE
1	Ac-Ser-Tyr-Ser- Met ⁴ -Glu ⁵ -His – Phe ⁷ -Arg-Trp -Gly-Lys-Pro-Val-NH ₂ (α-MSH)
2	Ac- Nle ⁴ -c[Asp ⁵ -His- DPhe ⁷ -Arg-Trp-Lys]-NH ₂ (MTII)
3	L¹⁸ - β Ala ³ -Nle ⁴ -c[Asp ⁵ -His- DPhe ⁷ -Arg-Trp-Lys]-NH ₂ (cyclic)
4	L¹⁸ - β Ala ³ -Nle ⁴ -Asp ⁵ -His- DPhe ⁷ -Arg-Trp-Lys-NH ₂ (linear)
5	Ac-Nle ⁴ -Asp ⁵ -His- DPhe ⁷ -Arg-Trp-Gly-Lys-NH ₂ (NAPamide)
6	Ac-Nle ⁴ -Asp ⁵ -His- DPhe ⁷ -Arg-Trp-Gly-Lys(L¹⁸)-NH ₂

The peptide conjugates (final concentration $\sim 1\text{-}5 \times 10^{-5}$ M) reacted with the precursor *fac*- $[^{99m}\text{Tc}(\text{CO})_3(\text{H}_2\text{O})]^+$, yielding (> 95%) stable radioactive complexes of the type $[^{99m}\text{Tc}(\text{CO})_3\text{-L}]^+$ (L = **L¹⁸**- β Ala³-Nle⁴-c[Asp⁵-His-**DPhe**⁷-Arg-Trp-Lys]-NH₂, (**28a**); **L¹⁸**- β Ala³-Nle⁴-Asp⁵-His-**DPhe**⁷-Arg-Trp-Lys-NH₂, (**29a**); and Ac-Nle⁴-Asp⁵-His-**DPhe**⁷-Arg-Trp-Gly-Lys(**L¹⁸**)-NH₂, (**30a**)).

The degree of internalization and cellular retention in B16F1 murine melanoma cells was used as a parameter for prediction of the tumor-targeting properties of the different radiopeptides. Higher levels of internalization were reached for the $^{99m}\text{Tc}(\text{CO})_3$ -labeled cyclic conjugate, compared with the linear analogs. Negligible amounts of radioactivity were internalized after 4 h for the linear radiopeptides ((**29a**): 1.6%; (**30a**): 5.4%), but remarkable internalization (50.5%, 4 h) was attained for the cyclic radioconjugate (**28a**). The latter internalization level is particularly high when compared with data previously reported for other radiolabeled α -MSH analogs, namely for the cyclic radiopeptide ^{99m}Tc -CCMSH that showed a lower internalization (< 4%) under the same experimental conditions [55].

Biodistribution studies in melanoma-bearing C57BL6 mice have shown that the cyclic radioconjugate (**28a**) presents a significant MC1R-mediated tumor uptake (9.26 ± 0.83 and $11.31 \pm 1.83\%$ ID/g at 1 and 4 h postinjection, respectively), as confirmed by receptor-blocking studies with the potent (Nle⁴,DPhe⁷)- α MSH agonist. The linear ^{99m}Tc(CO)₃-labeled peptide conjugates presented significantly lower tumor uptake values ((**29a**): $0.99 \pm 0.08\%$ ID/g at 4 h postinjection; (**30a**): $4.24 \pm 0.94\%$ ID/g, at 4 h postinjection). Despite the excellent tumor-targeting properties exhibited by the cyclic radiopeptide, improvement of its pharmacokinetic profile is needed to decrease kidney uptake and to increase the overall excretion. To achieve such goal the modification of the cyclic peptide conjugate is underway.

3.3 – Peptide Nucleic Acids

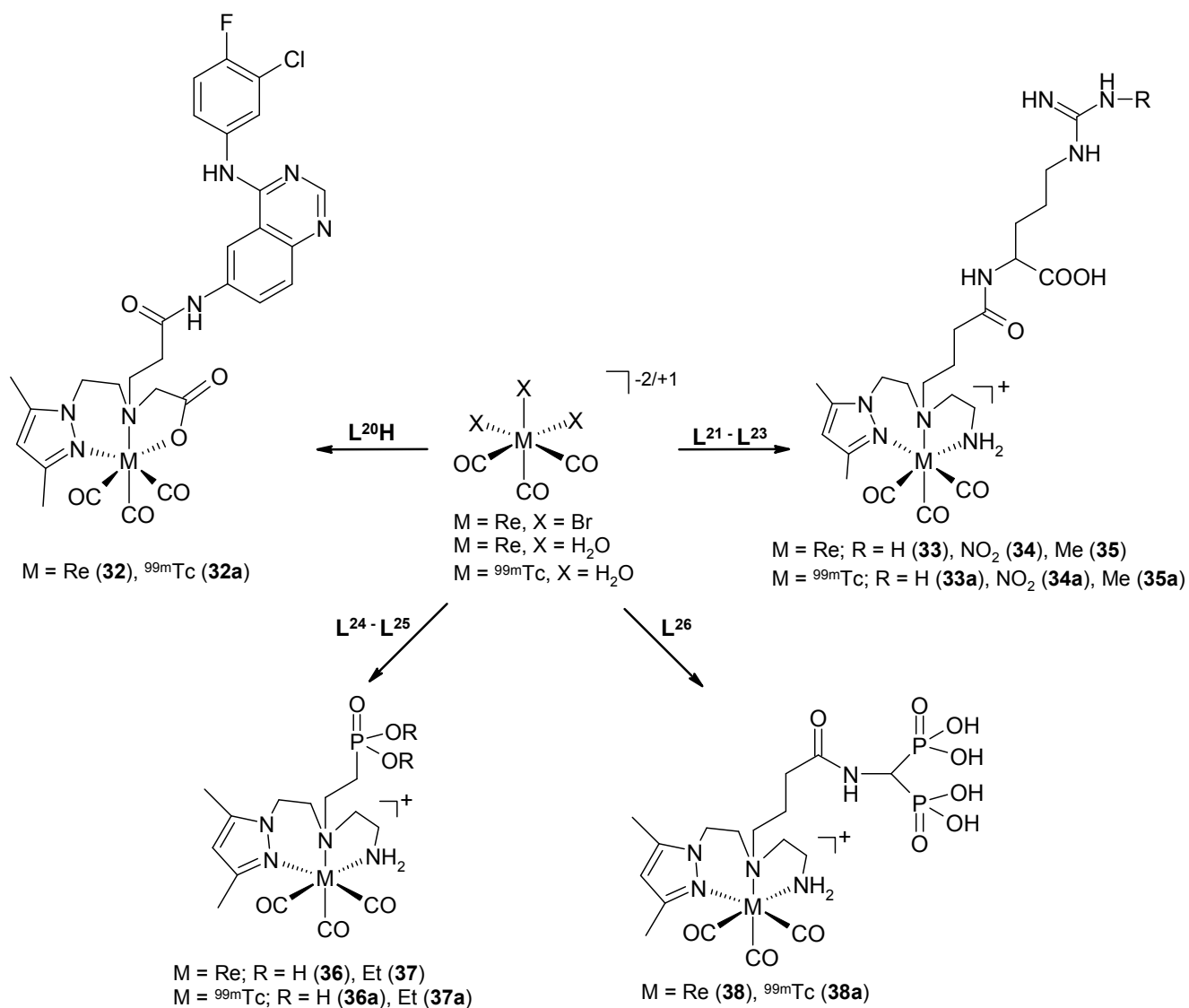
Peptide Nucleic acids (PNAs) are DNA analogs in which the sugar–phosphate backbone has been replaced by a pseudopeptide chain constituted by N-(2-aminoethyl)glycine [65-69]. PNAs are achiral, neutral, and stable over a wide range of pH, resistant to enzymatic degradation, and do not activate RNase H degradation of mRNA. They can also bind to complementary DNA/RNA, resulting in hybrid PNA/DNA or PNA/RNA duplexes which are thermodynamically more stable than the homoduplexes [65-69]. In the past few years, PNAs and their derivatives have been used as potential drugs, or as components for designing radioactive probes for *in vivo* imaging of endogenous gene expression through the antisense strategy [70, 71]. The latter approach is directed to transcription of genes into messenger RNA (mRNA), using a complementary sequence of the target mRNA for imaging.

Aiming to explore the possibility of labeling clinically relevant PNA sequences with the organometallic core *fac*-[^{99m}Tc(CO)₃]⁺ using the tridentate bifunctional ligand **L**¹⁸, we synthesized and characterized the 16-mer peptide nucleic acid sequence H-AGAT CAT GCC CGG CAT-Lys-NH₂, complementary to the translation start region of the N-myc oncogene messenger RNA [72-77], and coupled it to **L**¹⁸,

the internalization of a rhodamine-conjugated PNA into neuroblastoma cells. The conjugation of a targeting specific vector to the radioconjugate is currently underway.

3.4. – Small Biomolecules

A set of $^{99m}\text{Tc(I)}$ “bioactive” complexes, which comprise tridentate chelating units derived from (L^{12}H) and (L^{18}) and pendant enzyme substrate/inhibitor ((L^{20}H) and (L^{21}) – (L^{23})) or bone-seeking agents ((L^{24}) – (L^{26})) for *in vivo* targeting of tumors and bone-associated diseases, respectively (**Scheme 14**).



Scheme 14 – $^{99m}\text{Tc(I)}$ / Re(I) -complexes bearing small biomolecules.

Tumour imaging of EGFR receptors with radioactive probes has been a field of intense research in the past few years, namely based on tyrosine kinase inhibitors such as quinazoline derivatives [81 - 90]. Searching for useful ^{99m}Tc probes for early detection and staging of EGFR positive tumors, we have coupled the quinazoline pharmacophore (3-chloro-4-fluorophenyl)quinazoline-4,6-diamine to a tailor-made N_2O -tridentate chelator (L^{20}H) derived from L^{12} (Scheme 7) [91-93]. The corresponding ^{99m}Tc -complex (**32a**) was obtained in quantitative yield and with high radiochemical purity after optimization of the labeling conditions (Scheme 14).

In vitro studies confirmed that the corresponding Re complex (**32a**) still inhibits significantly the EGFR autophosphorylation and also inhibited A431 cell growth. Biodistribution studies with the ^{99m}Tc complex in healthy and tumor-bearing mice are currently in progress to prove their usefulness as a tumor imaging agent.

Nitric oxide synthase (NOS) is the eukaryotic enzyme responsible for the endogenous catalytic oxidation of L-arginine to L-citrulline. This reaction generates nitric oxide (NO), a key signaling mammalian mediator in several physiological processes, such as vasodilation, thermoregulation, neurotransmission and host-defence [94, 95]. The enzyme presents three isoforms (neuronal NOS, Nnos; endothelial NOS, eNOS; and inducible NOS, iNOS). Insufficient NO bioavailability from eNOS and nNOS is associated with hypertension, impotence, atherosclerosis and cardiovascular disease, whereas overproduction of NO from nNOS and iNOS has been associated to Alzheimer's and Parkinson's diseases [96-98]. Overproduction of NO by iNOS has also been linked to multiple sclerosis, inflammation, rheumatoid arthritis, stroke and cancer [96-98]. The *in vivo* imaging of NOS expression using radiolabeled NOS substrates/inhibitors, holds great potential for providing an insight into the wide variety of diseases linked to abnormal NO production [99 - 101]. Thus, aiming to design radioactive compounds based on the core " $^{99m}\text{Tc}(\text{CO})_3$ " for probing nitric oxide synthase (iNOS) levels *in vivo*, we have synthesized the bioconjugates (L^{21}) – (L^{23}) derived from (L^{18}), which contain the

pyrazolyl-diamine chelating unit and pendant L-arginine analogues (substrates and inhibitors of NOS) [102]. Reaction of (**L**²¹) – (**L**²³) with *fac*-[M(CO)₃]⁺ (M = Re, ^{99m}Tc) gave bioorganometallic complexes of the type *fac*-[M(CO)₃(k³-L)] (L = (**L**²¹), (**33**)/(**33a**); (**L**²²), (**34**)/(**34a**); (**L**²³), (**35**)/(**35a**)) in good yield (Scheme 14) [102]. After *in vitro* testing using the oxyhemoglobin NO capture assay, we concluded that the affinity of the inhibitor-containing conjugates to iNOS seems to be less affected upon metallation with rhenium than the substrate-containing conjugates. The rhenium complexes bearing guanidine-substituted analogues of L-arginine still present considerable inhibitory action ((**34**): K_i = 84 μM, R = N^ω-nitro-L-arginine; (**35**): K_i = 36 μM, R = N^ω-monomethyl-L-arginine), being the first examples of organometallic complexes able to inhibit the iNOS (Scheme 14) [102].

Taken together, the enzymatic studies and the high stability shown by the radioactive complexes revealed that “^{99m}Tc(CO)₃-labeled” L-arginine analogues, mainly NOS inhibitors, may hold great potential for monitoring increased levels of iNOS *in vivo*. Biological assessment of these compounds in specific cell lines with localized iNOS expression (*e.g.* lipopolysaccharide-activated macrophages) and specific animal models is underway.

The ^{99m}Tc-labeled bisphosphonates (^{99m}Tc-BP) routinely used for bone imaging (^{99m}Tc-MDP, MDP = methylenediphosphonate, and ^{99m}Tc-HMDP, HMDP = hydroxymethylenediphosphonate) present several drawbacks, such as *in vivo* instability, and relatively slow blood and soft-tissue clearance, delaying the start of the bone-scanning procedure in nuclear medicine centers [103 - 107]. From a chemical point of view, these ^{99m}Tc-BP radiopharmaceuticals do not present single, well-defined chemical species, but mixtures of short-chain and long-chain polymers, which may reduce the efficacy of the radiopharmaceutical [105]. Taken together, these disadvantages show that there is still space for the development of new bone-seeking radiotracers based on ^{99m}Tc with better chemical and biological properties. Therefore, aimed at developing new bone-seeking radiotracers based on the organometallic core *fac*-[^{99m}Tc(CO)₃]⁺ with improved properties, we have prepared the new phosphonate-containing

conjugates (**L**²⁴) – (**L**²⁶) which bear the pyrazolyl-diamine chelating unit [22]. Reactions of these chelators with the precursor [^{99m}Tc(H₂O)₃(CO)₃]⁺ yielded (> 95%) the single and well-defined complexes (**36a**) – (**38a**) (**Scheme 14**). The corresponding Re surrogates ((**36**) – (**38**)), characterized by the usual analytical techniques, including X-ray diffraction analysis in the case of (**37**), allowed for the chemical identification of the radioactive conjugates.

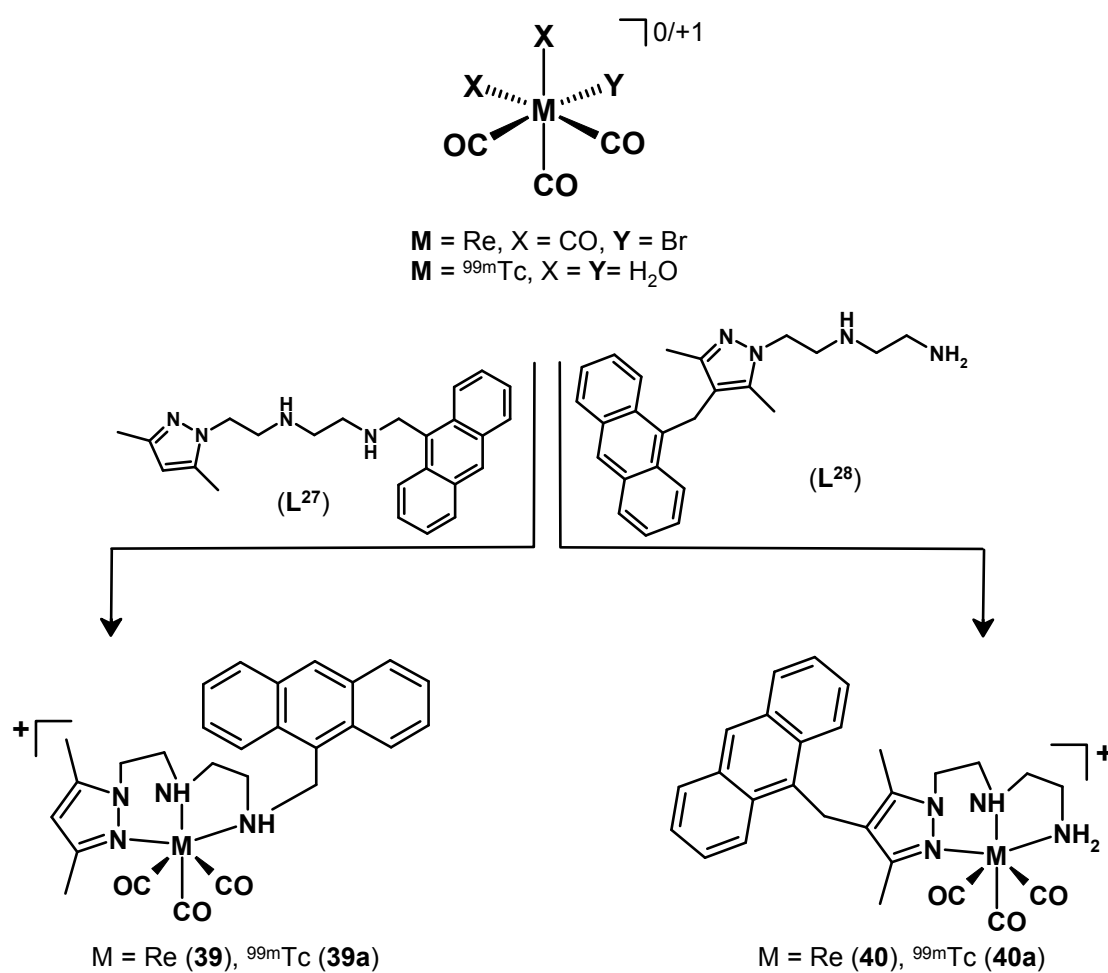
Complexes (**36a**) – (**38a**) revealed high stability both *in vitro* (phosphate-buffered saline solution and human plasma) and *in vivo*, without any measurable decomposition. Biodistribution studies of (**36a**) – (**38a**) in mice indicated a fast rate of blood clearance and high rate of total radioactivity excretion, occurring primarily through the renal–urinary pathway in the case of (**38a**). Despite presenting moderate bone uptake (3.04 ± 0.47% injected dose per gram of organ, 4 h after injection), the high stability presented by the latter radiocomplex and its adequate *in vivo* pharmacokinetics encourages the search for new ligands with the same chelating unit and different bisphosphonic acid pendant arms.

3.5 – DNA-Binders

^{99m}Tc-complexes may hold potential for targeted antitumor therapy since ^{99m}Tc is also an Auger-electron emitting radiometal. However, due to the short range of Auger electrons, there is a need for preferential accumulation of the complexes into the nucleus of the tumor cells in order to elicit significant DNA damage, and consequently a therapeutic effect [108,109]. Therefore, the improvement of the therapeutic efficiency of ^{99m}Tc requires the design of compounds having a better ability to target the nucleus. In this way, Alberto *et al.* have evaluated a ^{99m}Tc(I) tricarbonyl complex containing a pyrene intercalator and a NLS peptide, showing that this trifunctional complex can reach the nucleus of B16-F1 mouse melanoma cells, leading to much stronger radiotoxic effects compared with [^{99m}TcO₄]⁻. The same group has observed that related tricarbonyl ^{99m}Tc(I) or Re(I) complexes bearing acridine

orange as a DNA-binding group can also target the nucleus of murine B16F1 cells without needing a carrier NLS sequence [110-112].

With the goal of developing ^{99m}Tc radiopharmaceuticals for targeted radiotherapy, and taking advantage of the versatile nature of pyrazolyl-diamine chelators, we have introduced the novel ligands (L^{27}) and (L^{28}) that bear an anthracen-9-yl group as a DNA-binding fragment (Scheme 15) [113,114].



Scheme 15– Pyrazole-diamine chelators containing an anthracene chromophore and the corresponding organometallic complexes.

The evaluation of the coordination properties of (**L**²⁷) and (**L**²⁸) towards the *fac*-[M(CO)₃]⁺ moiety (M = ^{99m}Tc, Re) led to the preparation of the organometallic complexes (**39**)/(**39a**) and (**40**)/(**40a**) (Scheme 15) [113,114]. The interaction of the ligands (**L**²⁷) and (**L**²⁸), and respective rhenium complexes with calf thymus (CT) DNA has been investigated with a variety of spectroscopic techniques (UV-visible, fluorescence, circular dichroism (CD) and linear dichroism (LD)). All of the evaluated compounds have shown a moderate affinity to CT DNA ($3.46 \times 10^3 < K_b < 1.95 \times 10^4$), but the binding mode depends on the position of the chromophore in the framework of the pyrazolyl–diamine ligands. LD measurements have shown that (**L**²⁷) act as a DNA intercalator, but complex (**39**) intercalates only partially. By contrast, the compounds with the anthracenyl group at the 4-position of the azolyl ring ((**L**²⁸) and (**40**)) do not intercalate, and behave more like DNA groove binders. Independently of the mode of interaction with DNA, complexes (**39**) and (**40**) can reach the nucleus of murine B16-F1 cells, as demonstrated by fluorescence microscopy (Fig. (5)).

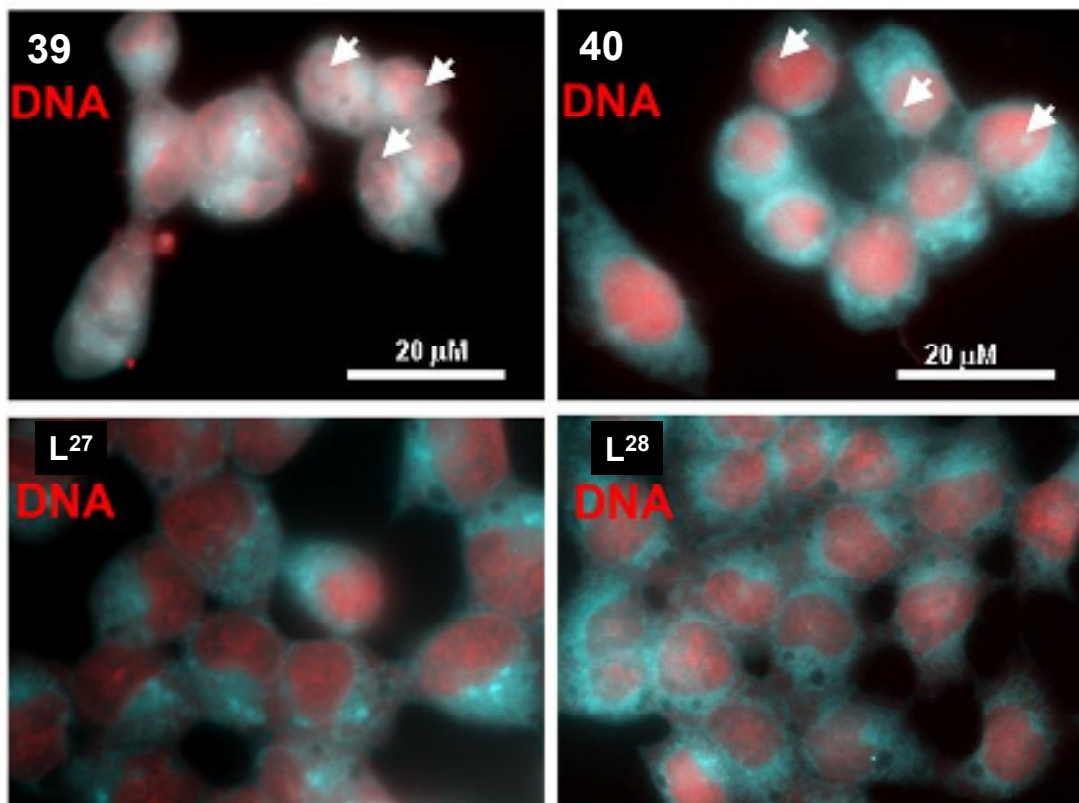


Fig. (5) - Fluorescence microscopy images of B16-F1 melanoma cells after 3 h of exposure to 80 μ M of complexes (**39**) or (**40**) (cyan colour in left and right top panels, respectively) and compounds (**L²⁷**) or (**L²⁸**) (cyan colour in left and right bottom panels, respectively), followed by fixation and DNA staining with DRAQ5 (red color in all panels).

The intracellular distribution and radiotoxicity of the ^{99m}Tc complexes, (**39a**) and (**40a**), were also evaluated using B16F1 murine melanoma cells. The radiotoxic effects depend very much on the position used to introduce the DNA binding group and are well correlated with the nuclear uptake of the compounds. Complex (**40a**), having the anthracenyl substituent at the 4-position of the pyrazolyl ring, rapidly entered the cells and accumulated inside the nucleus, exhibiting the highest radiotoxic effects. This compound induced an apoptotic cellular outcome, and its enhanced radiotoxic effects are certainly due to the Auger electrons emitted by the radiometal in close proximity to DNA. Hence, complex **40a** appear as a promising platform to be further explored in the design of biospecific ^{99m}Tc -complexes aiming at the further evaluation of the potential of ^{99m}Tc in targeted radiotherapy.

4 – Conclusions

The tetradentate pyrazolyl-containing N_3S -donor chelators did not emerge as promising compounds to be explored as bifunctional ligands for the labeling of biomolecules using $^{99m}\text{Tc(V)}$ oxocomplexes, mainly due to the unfavorable pharmacokinetic profile shown by the radioactive model complexes. In addition, the new N,N,O/O,O mixed-ligand oxorhenium(V) complexes were also inadequate for radiopharmaceutical applications since were quite unstable in the presence of thiol-containing molecules. The tridentate asymmetric pyrazolyl-containing chelators with N,N,N (neutral) or N,N,O (monoanionic) donor atom sets described herein presented relevant features (e.g. high stability, water solubility, easy functionalization and coordination possibilities) for the design of innovative $^{99m}\text{Tc(I)}$ -

based target-specific probes. Such versatility led to the preparation of a wide variety of well-defined cationic or neutral complexes of the type $fac-[M(CO)_3(k^3-L)]^{+/0}$ ($M = Re, {}^{99m}Tc$) in high yield. The ${}^{99m}Tc(I)$ model complexes, obtained in high radiochemical purity and high specific activity, were stable against cysteine and histidine exchange reactions and towards oxidation. These *in vitro* results, together with the adequate biological profile, namely high stability *in vivo* and fast clearance from blood and other main organs through the renal-urinary pathway, indicated that the chelators could be further explored in the design of bifunctional chelating ligands for the labeling of biomolecules. Our studies revealed that the functionalization of the model chelators through the central secondary amine, as well as through the pyrazolyl ring, did not change the coordination mode of the bifunctional chelators towards the tricarbonyl unit, and the biological properties of resulting complexes. Taking advantage of such properties, tumor-seeking peptides (bombesin and α -MSH analogs, and peptides containing the RGD sequence) and a peptide nucleic acid (PNA) have been conjugated to the chelators and labeled in high yield and high specific activity with the unit $fac-[{}^{99m}Tc(CO)_3]^+$. Despite exhibiting promising tumor-targeting properties, the pharmacokinetic profile of some of the labeled peptides has still to be further improved. Besides peptides, low molecular weight biomolecules such as quinazoline derivatives, bisphosphonates, L-arginine derivatives and DNA binders have also been labeled in high yield and high specific activity with retention of biological activity, as assessed using appropriate cell and animal models. In conclusion, the versatility of the pyrazolyl-containing chelators allowed the preparation of model ${}^{99m}Tc(I)$ complexes with different physico-chemical and biological properties for the labeling of a wide range of relevant biomolecules, spanning from small lipophilic organic molecules, such as quinazoline derivatives, to tumor-seeking peptides for *in-vivo* receptor targeting.

5 – Acknowledgements

We thank the Fundação para a Ciência e Tecnologia (PPCDT-POCI/SAU-FCF/58855/2004;XXXXXX) and Mallinkrodt-Tyco Inc. (MM) for financial support. MM is also acknowledged for providing the IsoLink[®] kits. The authors thank Carolina Moura for Molecular Structures drawing.

6 – References

- [1] – Saha, G.P. *Fundamentals of nuclear pharmacy*, Springer, New York, **2004**.
- [2] – Ametamey, S.M.; Honer, M.; Schubiger, P.A. Molecular imaging with PET. *Chem. Rev.*, **2008**, *108*, 1501–1516.
- [3] – Liu, S. Bifunctional coupling agents for radiolabeling of biomolecules and target-specific delivery of metallic radionuclides. *Adv. Drug Delivery Rev.*, **2008**, *60*, 1347-1370.
- [4] - Tisato, F.; Porchia M.; Bolzati, C.; Refosco, F.; Vittadini A. The preparation of substitution-inert Tc-99 metal-fragments: Promising candidates for the design of new Tc-99m radiopharmaceuticals. *Coord. Chem. Rev.*, **2006**, *250*, 2034-2045.
- [5] - Bandoli, G.; Tisato, F.; Dolmella, A; Agostini, S., Structural overview of technetium compounds (2000-2004). *Coord. Chem. Rev.*, **2006**, *250*, 561-573.
- [6] - Santos, I.; Paulo, A.; Correia, J.D.G. Rhenium and technetium complexes anchored by phosphines and scorpionates for radiopharmaceutical applications. *Top. Curr. Chem.*, **2005**, *252*, 45-84.
- [7] Santos, R.; Paulo, A.; Santos, I. Rhenium and technetium complexes with anionic or neutral scorpionates: An overview of their relevance in biomedical applications. *Inorg. Chim. Acta*, **2009**, doi:10.1016/j.ica.2009.06.034.
- [8] - Boschi, A.; Duatti, A.; Uccelli, L. Development of technetium-99m and rhenium-188 radiopharmaceuticals containing a terminal metal–nitrido multiple bond for diagnosis and therapy. *Top. Curr. Chem.*, **2005**, *252*, 85-115.

- [9] - Liu, S. 6-Hydrazinonicotinamide derivatives as bifunctional coupling Agents for ^{99m}Tc -Labeling of small biomolecules. *Top. Curr. Chem.*, **2005**, 252, 117-153.
- [10] - Alberto, R.; Schibli, R.; Egli, A.; Schubiger, A. P.; Abram, U.; Kaden, T. A. A novel organometallic aqua complex of technetium for the Labeling of biomolecules: Synthesis of $[\text{}^{99m}\text{Tc}(\text{OH}_2)_3(\text{CO})_3]^+$ from $[\text{}^{99m}\text{TcO}_4]^-$ in aqueous solution and its reaction with a bifunctional ligand. *J. Am. Chem. Soc.*, **1998**, 120, 7987–7988.
- [11] - Alberto, R. New organometallic technetium complexes for radiopharmaceutical imaging. *Top. Curr. Chem.*, **2005**, 252, 1-44.
- [12] - Alberto, R. The chemistry of technetium-water complexes within the manganese triad: challenges and perspectives. *Eur. J. Inorg. Chem.*, **2009**, 1, 21-31.
- [13] - Bartholoma, M.; Valliant, J.; Maresca, K.P.; Babich, J.; Zubieta, J. Single amino acid chelates (SAAC): a strategy for the design of technetium and rhenium radiopharmaceuticals. *Chem. Commun.*, **2009**, 5, 493-512
- [14] - Moura, C.; Vitor, R.F.; Maria, L.; Paulo, A.; Santos, I.C.; Santos, I. Rhenium(V) oxocomplexes with novel pyrazolyl-based N_4 - and N_3S -donor chelators. *Dalton Trans.*, **2006**, 5630 – 5640.
- [15] – Videira, M.; Silva, F.; Paulo, A.; Santos, I.C.; Santos, I. Synthesis and structural studies of mixed-ligand rhenium(V) complexes anchored by tridentate pyrazole-based ligands, *Inorg. Chim. Acta*, **2009**, 362, 2807 – 2813.
- [16] – Alves, S.; Paulo, A.; Correia, J.D.G.; Domingos, Â.; Santos, I. Coordination capabilities of pyrazolyl containing ligands towards the *fac*- $[\text{Re}(\text{CO})_3]^+$ moiety. *J. Chem. Soc., Dalton Trans.*, **2002**, 4714 – 4719.

[17] – Alves, S.; Paulo, A.; Correia, J.D.G.; Gano, L.; Santos, I. New building blocks for labeling peptides with the $[^{99m}\text{Tc}(\text{CO})_3]^+$ core. In *Technetium, Rhenium and other Metals in Chemistry and Nuclear Medicine 6*; Mazzi, U., Nicolini, M., Eds.; Proceedings of the sixth international symposium on technetium in chemistry and nuclear medicine; SGE Editoriali: Padova, Italy, 2002; pp 139-141.

[18] – Vitor, R.F.; Alves, S.; Correia, J.D.G.; Paulo, A.; Santos, I. Rhenium(I)- and technetium(I) tricarbonyl complexes anchored by bifunctional pyrazole-diamine and pyrazole-dithioether chelators. *J. Organomet. Chem.*, **2004**, *689*, 4764–4774.

[19] - Alves, S.; Paulo, A.; Correia, J.D.G.; Gano, L.; Smith, C.J.; Hoffman, T.J.; Santos, I. Pyrazolyl derivatives as bifunctional chelators for labeling tumor-seeking peptides with the *fac*- $[\text{M}(\text{CO})_3]^+$ moiety (M = ^{99m}Tc , Re): synthesis, characterization, and biological behavior. *Bioconjugate Chem.*, **2005**, *16*, 438-449

[20] - Moura, C.; Fernandes, C.; Gano, L.; Paulo, A.; Santos, I. Rhenium(I) and ^{99m}Tc technetium(I) tricarbonyl complexes anchored by monoanionic pyrazolyl-based chelators. In *Technetium, Rhenium and other Metals in Chemistry and Nuclear Medicine 7*, Mazzi, U., Ed.; Proceedings of the seventh international symposium on technetium in chemistry and nuclear medicine; SGE Editoriali: Padova, Italy, 2006; pp 101-102.

[21] - Moura, C.; Fernandes, C.; Gano, L.; Paulo, A., Santos, I.C.; Santos, I.; Calhorda, M. J. Influence of the ligand donor atoms on the in vitro stability of rhenium(I) and technetium (I)- ^{99m}Tc complexes with pyrazole-containing chelators: experimental and DFT studies. *J. Organomet. Chem.*, **2009**, *694*, 950 – 958.

- [22] - Palma, E.; Oliveira, B.L.; Correia, J.D.G.; Gano, L.; Maria, L., Santos, Maria, L.; Santos, I.C.; Santos, I. A new bisphosphonate-containing $^{99m}\text{Tc}(\text{I})$ tricarbonyl complex potentially useful as bone-seeking agent: synthesis and biological evaluation. *J. Biol. Inorg. Chem.*, **2007**, *12*, 667 – 679.
- [23] - Oliveira, B.L.; Figueira, F.; Morais, M.; Gano, L.; Santos, I.C.; Santos, I.; Correia, J.D.G, *unpublished results*.
- [24] - Palma, E.; Oliveira, B.L.; Figueira, F.; Correia, J.D.G.; Raposinho, P.D.; Santos, I. A pyrazolylamine-phosphonate monoester chelator for the *fac*- $[\text{M}(\text{CO})_3]^+$ core (M = Re, ^{99m}Tc): synthesis, coordination properties and biological assessment. *J. Label. Compd. Radiopharm.*, **2007**, *50*, 1176–1184.
- [25] – Wester, H.-J. Nuclear imaging probes: from bench to bedside. *Clin. Cancer Res.*, **2007**, *13*, 3470–3481.
- [26] – Weissleder, R.; Pittet, M.J. Imaging in the era of molecular oncology. *Nature*, **2008**, *452*, 580-589.
- [27] – Mather, S.J. Molecular imaging with bioconjugates in mouse models of cancer. *Bioconjugate Chem.*, **2009**, *20*, 631-643.
- [28] – Mather, S.J. Design of radiolabelled ligands for the imaging and treatment of cancer. *Mol. BioSyst.*, **2007**, *3*, 30-35.
- [29] – Reubi, J.C.; Maecke, H.R. Peptide-based probes for cancer imaging. *J. Nucl. Med.*, **2008**, *49*, 1735–1738.
- [30] – Schottelius, M.; Wester, H.-J. Molecular imaging targeting peptide receptors. *Methods*, **2009**, *48*, 161-177.

- [31] – Zaccaro, L.; del Gato, A.; Pedone, C.; Saviano M. Peptides for tumour therapy and diagnosis: current status and future directions. *Curr. Med. Chem.*, **2009**, *16*, 780-795.
- [32] – Kung, H.F.; Kung, M.P.; Wey, S.P.; Lin, K.J.; Yen, T.C. Clinical acceptance of a molecular imaging agent: a long march with [^{99m}Tc]TRODAT. *Nucl. Med. Biol.*, **2007**, *34*, 787-789.
- [33] - Mahmoud, S.; Staley, J.; Taylor, J.; Bogden, A.; Moreau, J.-P.; Coy, D.; Avis, I.; Cuttitta, F.; Mulshine, J.L.; Moody, T.W. [Psi^{13,14}] Bombesin analogues inhibit growth of small cell lung cancer in vitro and in vivo. *Life Sci.*, **1985**, *37*, 105-113.
- [34] - Qin, Y.; Ertl, T.; Cai, R.-Z.; Halmos, G.; Schally, A. V. Inhibitory effect of bombesin receptor antagonist RC-3095 on the growth of human pancreatic cancer cells in vivo and in vitro. *Cancer Res.* **1994**, *54*, 1035-1041.
- [35] - Qin, Y., Ertl, T.; Cai, R.-Z.; Horvath, J.E.; Groot, K.; Schally, A.V. Antagonists of bombesin/gastrin releasing peptide inhibit growth of SW-1990 human pancreatic adenocarcinoma and production of cyclic AMP. *Int. J. Cancer*, **1995**, *63*, 257-262.
- [36] - Plonowski, A.; Nagy, A.; Schally, A.V.; Sun, B.; Groot, K.; Halmos, G. In vivo inhibition of PC-3 human androgen-independent prostate cancer by a targeted cytotoxic bombesin analogue AN-215. *Int. J. Cancer*, **2000**, *88*, 652-657.
- [37] - Smith, C.J.; Volkert, W.A.; Hoffman, T.J. Radiolabeled peptide conjugates for targeting of the bombesin receptor superfamily subtypes. *Nucl. Med. Biol.*, **2005**, *32*, 733–740.
- [38] - Smith, C.J.; Volkert, W.A.; Hoffman, T.J. Gastrin releasing peptide (GRP) receptor targeted radiopharmaceuticals: a concise update. *Nucl. Med. Biol.*, **2003**, *30*, 861– 868.

- [39] - Giblin, M.F.; Veerendra, B.; Smith, C.J. Radiometallation of receptor specific peptides for diagnosis and treatment of human cancer. *In Vivo*, **2005**, *19*, 9 – 30.
- [40] – Fragogeorgi, E.A.; Zikos, C.; Gourni, E.; Bouziotis, P.; Paravatou-Petsotas, M.; Loudos, G.; Mitsokapas, N.; Xanthopoulos, S.; Mavri-Vavayanni, M.; Livaniou, E.; Varvarigou, A.D.; Archimandritis, S.C. Spacer site modifications for the improvement of the in vitro and in vivo binding properties of ^{99m}Tc -N₃S-X-Bombesin[2-14] derivatives. *Bioconjugate Chem.*, **2009**, *20*, 856 – 867.
- [41] - La Bella, R.; Garcia-Garayoa, E.; Langer M.; Blaustein, P.; Beck-Sickinger, A.G.; Schubiger, P.A. In vitro and in vivo evaluation of a ^{99m}Tc (I)-labeled bombesin analogue for imaging of gastrin releasing peptide receptor-positive tumors. *Nucl. Med. Biol.*, **2002**, *29*, 553–560.
- [42] - Alves, S.; Correia, J.D.G.; Santos, I.; Veerendra, B.; Sieckman, G.L.; Hoffman, T.J.; Rold, T.L.; Figueroa, S.D.; Retzlöff, L.; McCratea, J.; Prasanphanich, A.; Smith, C.J. Pyrazolyl conjugates of bombesin: a new tridentate ligand framework for the stabilization of *fac*-[M(CO)₃]⁺ moiety. *Nucl. Med. Biol.*, **2006**, *33*, 625 – 634.
- [43] - Haubner, R.; Decristoforo, C. Radiolabelled RGD peptides and peptidomimetics for tumour targeting. *Front. Biosci.* **2009**, *14*, 872-886.
- [44] - Haubner, R.H.; Wester H.J.; Weber, W.A.; Schwaiger, M. Radiotracer-based strategies to image angiogenesis. *Q. J. Nucl. Med. Biol.*, **2003**, *47*, 189-199.
- [45] - Haubner, R. $\alpha_v\beta_3$ -integrin imaging: A new approach to characterise angiogenesis? *Eur. J. Nucl. Med. Mol. Imaging*, **2006**, *33* Suppl. 1, S54-S63.
- [46] - Haubner, R.; Wester, H.J. Radiolabeled tracers for imaging of tumor angiogenesis and evaluation of anti-angiogenic therapies. *Curr. Pharm. Des.*, **2004**, *10*, 1439-1455.

- [47] - Healy, J.M.; Murayama, O.; Maeda, T.; Yoshino, K.; Sekiguchi, K.; Kikuchi, M.M. Peptide ligands for integrin $\alpha_v\beta_3$ selected from random phage display libraries. *Biochemistry*, **1995**, *34*, 3948-3955.
- [48] - Reinmuth, N.; Liu, W.; Ahmad, S.A.; Fan, F., Stoeltzing; O., Parikh, A.A.; Bucana, C.D.; Gallick, G.E.; Nickols, M.A.; Westlin, W.F.; Ellis, L.M. $\alpha_v\beta_3$ integrin antagonist S247 decreases colon cancer metastasis and angiogenesis and improves survival in mice. *Cancer Res.*, **2003**, *63*, 2079-2087.
- [49] - Kerr, J.S.; Slee, A.M.; Mousa, S.A. Small molecule α_v integrin antagonists: novel anticancer agents. *Exp. Opin. Invest. Drugs*, **2000**, *9*, 1271-1279.
- [50] - Alves, S.; Correia, J.D.G.; Gano, L.; Rold, T.L.; Prasanphanich, A.; Haubner, R.; Rupprich, M; Alberto, R.; Decristoforo, C.; Santos, I.; Smith, C.J. In vitro and in vivo evaluation of a novel $^{99m}\text{Tc}(\text{CO})_3$ -pyrazolyl conjugate of cyclo-(Arg-Gly-Asp-D-Tyr-Lys). *Bioconjugate Chem.*, **2007**, *18*, 530 – 537.
- [51] - Decristoforo, C.; Santos, I.; Pietzsch, H.-J; Kuenstler, J.U.; Duatti, A.; Smith, C.J.; Rey, A.; Alberto, R.; Von Guggenberg, Haubner, R. Comparison of *in vitro* and *in vivo* properties of [^{99m}Tc]cRGD peptides labeled using different novel Tc-cores. *Q. J. Nucl. Med. Biol. Mol. Imag.*, **2007**, *51*, 33 – 41.
- [52] - Ghanem, G.E.; Comunale, G.; Libert A.; Vercammen-Grandjean, A.; Lejeune, F.J. Evidence for alpha-melanocyte-stimulating hormone (alpha-MSH) receptors on human malignant melanoma cells. *Int. J. Cancer*, **1988**, *41*, 248 – 255.

- [53] - Siegrist, W.; Solca, F.; Stutz, S.; Giuffre, L.; Carrel, S.; Girard, J.; Eberle A.N. Characterization of receptors for alpha-melanocyte-stimulating hormone on human melanoma cells. *Cancer Res.*, **1989**, *49*, 6352 – 6358.
- [54] - Siegrist, W.; Stutz, S; Eberle, A.N. Homologous and heterologous regulation of α -melanocyte-stimulating hormone receptor in human and mouse melanoma cell lines. *Cancer Res.*, **1994**, *54*, 2604–2610.
- [55] - Chen, J.-Q; Chen, Z.; Hoffman, T.J.; Jurisson, S.S.; Quinn, T.P. melanoma targeting properties of ^{99m}Tc -labeled cyclic alpha-melanocyte stimulating hormone peptide analogs. *Cancer Res.*, **2000**, *60*, 5649 – 5658.
- [56] - Miao, Y.; Hoffman, T.J.; Quinn, T.P. Tumor-targeting properties of ^{90}Y - and ^{177}Lu -labeled α -melanocyte stimulating hormone peptide analogues in a murine melanoma model. *Nucl. Med. Biol.* **2005**, *32*, 485 – 493.
- [57] - Wei, L.; Butcher, C.; Miao, Y., Gallazzi F.; Quinn, T.P.; Welch, M.J.; Lewis, J.S.; Synthesis and biologic evaluation of ^{64}Cu -labeled rhenium-cyclized α -MSH peptide analog using a cross-bridged cyclam chelator. *J. Nucl. Med.*, **2007**, *48*, 64–72.
- [58] - Miao Y, Benwell K, Quinn TP. ^{99m}Tc -and ^{111}In -labeled α -melanocyte stimulating hormone peptides as imaging probes for primary and pulmonary metastatic melanoma detection. *J. Nucl. Med.* **2007**, *48*, 73–80.
- [59] - Miao, Y.; Owen, N.K.; Fisher, D.R.; Hoffman, T.J.; Quinn, T.P. Therapeutic efficacy of a ^{188}Re -labeled-melanocyte–stimulating hormone peptide analog in murine and human melanoma-bearing mouse models. *J. Nucl. Med.*, **2005**, *46*, 121-129.

- [60] - Miao, Y.; Hylarides, M.; Fisher, D.R.; Shelton, T.; Moore, H.; Wester, D.W.; Fritzberg, A.R.; Winkelmann, C. T.; Hoffman, T.J.; Quinn, T. P. Melanoma therapy via peptide-targeted-radiation. *Clin. Cancer Res.*, **2005**, *11*, 5616 - 5621.
- [61] - McQuade, P; Miao, Y; Yoo, J.; Quinn, T.P., Welch, M.J.; Lewis, J.S. Imaging of Melanoma Using ^{64}Cu - and ^{86}Y -DOTA-ReCCMSH(Arg¹¹), A cyclized peptide analogue of α -MSH. *J. Med. Chem.*, **2005**, *48*, 2985 – 2992.
- [62] - Valldosera, M.; Monso, M.; Xavier, C.; Raposinho, P.D.; Correia, J.D.G.; Santos, I.; Gomes, P Comparative study of chemical approaches to the solid-phase synthesis of a tumor-seeking α -MSH analogue. *Int. J. Pept. Res. Ther.*, **2008**, *14*, 273–281.
- [63] - Raposinho, P.D.; Xavier, C.; Correia, J.D.G.; Falcão, S.; Gomes, P.; Santos, I. Melanoma targeting with α -melanocyte stimulating hormone analogs labeled with $fac\text{-}[^{99\text{m}}\text{Tc}(\text{CO})_3]^+$: effect of cyclization on tumor-seeking properties. *J. Biol. Inorg. Chem.*, **2008**, *13*, 449 – 459.
- [64] - Raposinho, P.D.; Correia, J.D.G.; Alves, S., Botelho, M.F.; Santos, A.C.; Santos, I. A $^{99\text{m}}\text{Tc}(\text{CO})_3$ -labeled pyrazolyl- α -melanocyte-stimulating hormone analog conjugate for melanoma targeting. *Nucl. Med. Biol.*, **2008**, *35*, 91 – 99.
- [65] - Kumar, A. structural preorganization of peptide nucleic acids: chiral cationic analogues with five- or six-membered ring Structures. *Eur. J. Org. Chem.*, **2002**, *13*, 2021 - 2032.
- [66] - Basu, S.; Wickstrom, E. Synthesis and characterization of a peptide nucleic acid conjugated to a D-peptide analog of insulin-like Growth Factor 1 for increased cellular uptake. *Bioconjugate Chem.*, **1997**, *8*, 481 - 488.

- [67] - Menchise, V.; De Simone, G.; Tedeschi, T.; Corradini, R.; Sforza, S.; Marchelli, R.; Capasso, D.; Saviano, M.; Pedone C. Insights into peptide nucleic acid (PNA) structural features: The crystal structure of a d-lysine-based chiral PNA–DNA duplex. *P. Natl. Acad. Sci.*, **2003**, *100*, 12021 – 12026.
- [68] - Rasmussen, H.; Kastrup, J.S.; Nielsen, J.N.; Nielsen, J.M.; Nielsen, P.E. Crystal structure of a peptide nucleic acid (PNA) duplex at 1.7 Å resolution. *Nat. Struct. Biol.*, **1997**, *4*, 98 – 101.
- [69] - Ray, A.; Nordén, B. Peptide nucleic acid (PNA): its medical and biotechnical applications and promise for the future. *FASEB J.*, **2000**, *14*, 1041 - 1060.
- [70] - Hnatowich, D.J.; Nakamura, K. Antisense targeting in cell culture with radiolabeled DNAs - a brief review of recent progress. *Ann. Nucl. Med.*, **2004**, *18*, 363 – 368.
- [71] - Sun, X.; Fang, H.; Li, X.; Rossin, R.; Welch, M.J.; Taylor, J.-S. MicroPET imaging of MCF-7 tumors in mice via unr mRNA-targeted peptide nucleic Acids. *Bioconjugate Chem.*, **2005**, *16*, 294 – 305.
- [72] - Stanton, L.W.; Schwab, M.; Bishop, J.M. Nucleotide sequence of the human N-myc gene. *Proc. Natl. Acad. Sci. USA*, **1986**, *83*, 1772–1776.
- [73] - Tonelli, R.; Purgato, S.; Camerin, C.; Fronza, R.; Bologna, F.; Alboresi, S.; Franzoni, M.; Corradini, R.; Sforza, S.; Faccini, A.; Shohet, J.M.; Marchelli, R.; Pession, A. Anti-gene peptide nucleic acid specifically inhibits *MYCN* expression in human neuroblastoma cells leading to cell growth inhibition and apoptosis. *Mol. Cancer Ther.*, **2005**, *4*, 779 – 786.
- [74] - Watanabe, N.; Sawai, H.; Ogihara-Umeda, I.; Tanada, S.; Kim, E.E.; Yonekura, Y.; Sasaki, Y. Molecular therapy of human neuroblastoma cells using Auger electrons of ¹¹¹In-Labeled N-myc antisense oligonucleotides. *J. Nucl. Med.*, **2006**, *47*, 1670–1677.

- [75] - Pession, A.; Tonelli, R.; Fronza, R.; Sciamanna, E.; Corradini, R.; Sforza, S.; Tedeschi, T.; Marchelli, R.; Montanaro, L.; Camerin, C.; Franzoni, M.; Paolucci, G. Targeted inhibition of NMYC by peptide nucleic acid in N-myc amplified human neuroblastoma cells: cell-cycle inhibition with induction of neuronal cell differentiation and apoptosis. *Int. J. Oncol.*, **2004**, *24*, 265–272.
- [76] - Giles, R.H.; Shaw, P.J.; Uren, R.F.; Chung, D.K.V. Neuroblastoma and other neuroendocrine tumors. *Semin. Nucl. Med.*, **2007**, *37*, 286 – 302.
- [77] - Nau, M.M.; Brooks, B.J.; Carney, D.N.; Gazdar, A.F.; Battey, J.F.; Sausville, E.A.; Minna, J.D. Human small-cell lung cancers show amplification and expression of the N-myc gene. *Proc. Natl. Acad. Sci. USA*, **1986**, *83*, 1092–1096.
- [78] - Xavier, C.; Giannini, C.; Gano, L.; Maiorana, S.; Alberto, R.; Santos, I. Synthesis, characterization, and evaluation of a novel $^{99m}\text{Tc}(\text{CO})_3$ pyrazolyl conjugate of a peptide nucleic acid sequence. *J. Biol. Inorg. Chem.*, **2008**, *13*, 1335–1344.
- [79] - Xavier, C.; Santos, I.; Alberto, R. Synthesis, characterization and stability studies of Re(I) and $^{99m}\text{Tc}(\text{I})$ tricarbonyl complexes bearing a PNA dimer. In *Technetium, Rhenium and other Metals in Chemistry and Nuclear Medicine 7*, Mazzi, U., Ed.; Proceedings of the seventh international symposium on technetium in chemistry and nuclear medicine; SGE Editoriali: Padova, Italy, 2006; pp 371-376.
- [80] - Xavier, C.; Pak, J.-K.; Santos, I.; Alberto, R. Evaluation of two chelators for labelling a PNA monomer with the *fac*- $^{99m}\text{Tc}(\text{CO})_3^+$ moiety. *J. Organomet. Chem.* **2007**, *692*, 1332–1339.
- [81] - Laskin, J.J.; Sandler, A.B. Epidermal growth factor receptor: a promising target in solid tumours. *Cancer Treat. Rev.*, **2004**, *30*, 1 – 17.

- [82] - Bianco, R.; Gelardi, T.; Damiano, V.; Ciardiello, F.; Tortora, G. Rational bases for the development of EGFR inhibitors for cancer treatment. *Int. J. Biochem. Cell Biol.*, **2007**, *39*, 1416 – 1431.
- [83] - Zandi, R.; Larsen, A.B.; Andersen, P.; Stockhausen, M.-T.; Poulsen, H.S. Mechanisms for oncogenic activation of the epidermal growth factor receptor. *Cell. Signalling*, **2007**, *19*, 2013 – 2023.
- [84] - Arteaga, C. Targeting HER1/EGFR: a molecular approach to cancer therapy. *Semin. Oncol.*, **2003**, *30/7*, 3 – 14.
- [85] - Mass, R.D. The HER receptor family: a rich target for therapeutic development, *Int. J. Radiat. Oncol., Biol., Phys.*, **2004**, *58*, 932 – 940.
- [86] - Albanell, J.; Gascon, P. Small Molecules with EGFR-TK inhibitor activity, *Curr. Drug Targets*, **2005**, *6*, 259 – 274.
- [87] - Cai, W.; Niu, G.; Chen, X. Multimodality imaging of the HER-kinase axis in cancer. *Eur. J. Nucl. Med. Mol. Imaging*, **2008**, *35*, 186 – 208.
- [88] - Ortu, G.; Ben-David, I.; Rozen, Y.; Freedman, N.M.T. Chisin, R.; Levitzki, A.; Mishani, E. Labeled EGFR-TK irreversible inhibitor (ML03): In vitro and in vivo properties, potential as PET biomarker for cancer and feasibility as anticancer drug. *Int. J. Cancer*, **2002**, *101*, 360 – 370.
- [89] - Abourbeh, G.; Dissoki, S.; Jacobson, O.; Litchi, A.; Daniel, R.B.; Laki, D.; Levitzki, A.; Mishani, E. Evaluation of radiolabeled ML04, a putative irreversible inhibitor of epidermal growth factor receptor, as a bioprobe for PET imaging of EGFR-overexpressing tumors. *Nucl. Med. Biol.*, **2007**, *34*, 55 – 70.

- [90] - Shaul, M.; Abourbeh, G.; Jacobson, O.; Rozen, Y.; Desideriu, L.; Levitzki, A.; Mishani, E. Novel iodine-124 labeled EGFR inhibitors as potential PET agents for molecular imaging in cancer. *Bioorg. Med. Chem.*, **2004**, *12*, 3421 – 3429.
- [91] - Fernandes, C.; Gano, L.; Bourkoula, A.; Pirmettis, I.; Santos, I. Novel Re(I)/^{99m}Tc(I) tricarbonyl complexes bearing quinazoline moiety as biomarkers for epidermal growth factor receptor positive tumors. In *Technetium, Rhenium and other Metals in Chemistry and Nuclear Medicine 7*, Mazzi, U., Ed.; Proceedings of the seventh international symposium on technetium in chemistry and nuclear medicine; SGE Editoriali: Padova, Italy, 2006; pp 487-490.
- [92] - Margaritis, N.; Bourkoula, A.; Chiotellis, A.; Papadopoulos, A.; Panagiotopoulou, A.; Tsoukalas, C.; Fernandes, C.; Pelecanou, M.; Paravatou, M.; Livaniou, E.; Santos, I.; Papadopoulos, M.; Pirmettis, I. A new technetium-99m biomarker for EGFR-TK. In *Technetium, Rhenium and other Metals in Chemistry and Nuclear Medicine 7*, Mazzi, U., Ed.; Proceedings of the seventh international symposium on technetium in chemistry and nuclear medicine; SGE Editoriali: Padova, Italy, 2006; pp 523-524.
- [93] - Fernandes, C.; Santos, I.C.; Santos, I.; Pietzsch, H.-J.; Kunstler, J.-U.; Kraus, W.; Rey, A.; Margaritis, N.; Bourkoula, A.; Chiotellis, A.; Paravatou, M.; Pirmettis, I. Rhenium and technetium complexes bearing quinazoline derivatives: progress towards a ^{99m}Tc biomarker for EGFR-TK imaging. *Dalton Trans.*, **2008**, 3215–3225.
- [94] – Kerwin, J.F.; Lancaster, J.R.; Feldman, P.L. Nitric oxide – a new paradigm for second messengers. *J. Med. Chem.*, **1995**, *38*, 4343 - 4362.
- [95] - Moncada, S.; Palmer, R.M.J.; Higgs, E.A. Nitric oxide: physiology, pathophysiology, and pharmacology. *Pharmacol. Rev.* **1991**, *43*, 109 - 142.

- [96] – Korhonen, R.; Lahti, A.; Kankaanranta, H.; Moilanen, E. Nitric oxide production and signaling in inflammation. *Curr. Drug Targets Inflamm. Allergy*, **2005**, *4*, 471 – 479.
- [97] – Fukumura, D.; Kashiwagi, S.; Jain, R.K. The role of nitric oxide in tumour progression, *Nat. Rev. Cancer*, **2006**, *6*, 521 - 534.
- [98] - Duncan, A.J.; Heales, S.J. Nitric oxide and neurological disorders. *Mol. Aspects Med.*, **2005**, *26*, 67 - 96.
- [99] - Zhang, J.; Xu, M.; Dence, C.S.; Sherman, E.L.C.; MacCarthy, T.J.; Welch, M.J. Synthesis, *in vivo* evaluation and PET study of a carbon-11-labeled neuronal nitric oxide synthase (nNOS) inhibitor S-Methyl-L-thiocitrulline. *J. Nucl. Med.*, **1997**, *38*, 1273 - 1278.
- [100] - Zhang, J.; McCarthy, T.J.; Moore, W.M.; Currie, M.G.; Welch, M.J. Synthesis and evaluation of two positron-labeled nitric oxide synthase inhibitors, S-[C-11]methylisothiourea and S-(2-[F-18]fluoroethyl)isothiourea, as potential positron emission tomography tracers. *J. Med. Chem.*, **1996**, *39*, 5110 - 5118.
- [101] - Zhou, D.; Lee, H.; Rothfuss, J.M.; Chen, D.L.; Ponde, D. E.; Welch, M.J.; Mach, R.H. Design and synthesis of 2-Amino-4-methylpyridine analogues as inhibitors for inducible nitric oxide synthase and *in vivo* evaluation of [¹⁸F]6-(2-Fluoropropyl)-4-methyl-pyridin-2-amine as a potential PET tracer for inducible nitric oxide synthase. *J. Med. Chem.*, **2009**, *52*, 2443 – 2453.
- [102] - Oliveira, B.L.; Correia, J.D.G.; Raposinho, P.D.; Santos, I.; Ferreira, A.; Cordeiro, C.; Freire, A.P. Re and ^{99m}Tc organometallic complexes containing pendant L-arginine derivatives as potential probes of inducible nitric oxide synthase. *Dalton Trans.*, **2009**, 152 – 162.

- [103] - Love, C.; Din, A.S.; Tomas, M.B.; Kalapparambath, T.P.; Palestro, C.J. Radionuclide bone imaging: an illustrative review. *Radiographics*, **2003**, *23*, 341 – 358.
- [104] - Zhang, S.; Gangal, G.; Uluda, H.; Magic bullets for bone diseases: progress in rational design of bone-seeking medicinal agents. *Chem. Soc. Rev.*, **2007**, *36*, 507 – 531.
- [105] - Verbeke, K.; Rozenski, J.; Cleynhens, B.; Vanbilloen, H.; Groot, T.; Weyns, N.; Bormans, G.; Verbruggen, A., Development of a conjugate of ^{99m}Tc -EC with aminomethylenediphosphonate in the search for a bone tracer with fast clearance from soft tissue, *Bioconjugate Chem.*, **2002**, *13*, 16 – 22.
- [106] - Doubisky, J.; Laznicek, M.; Laznickova, A.; Leseticky, L. Phosphonate complexes of ^{99m}Tc - Potential bone scintigraphy agents. *J. Radioanal. Nucl. Chem.*, **2004**, *260*, 53 – 59.
- [107] - Liu, J.; Wang, F.L.; Zhang, J.B.; Yang, S.Y.; Guo, H.X.; Wang, X.B. Synthesis, characterization and biodistribution of $^{99m}\text{Tc}(\text{CO})_3\text{-ABP}$ and comparison with $^{99m}\text{Tc-ABP}$. *J. Label. Compd. Radiopharm.*, **2007**, *50*, 1243 – 1247.
- [108] - Kassis, A. I. Cancer therapy with Auger electrons: Are we almost there? *J. Nucl. Med.*, **2003**, *44*, 1479 – 1481.
- [109] - Ginj, M.; Hinni, K.; Tschumi, S.; Schulz, S.; Maecke, H. Trifunctional somatostatin-based derivatives designed for targeted radiotherapy using Auger electron emitters. *J. Nucl. Med.*, **2005**, *46*, 2097 – 2103.
- [110] - Haefliger, P.; Agorastos, N.; Spingler, B.; Georgiev, O.; Viola, G.; Alberto, R. Induction of DNA-double-strand breaks by Auger electrons from ^{99m}Tc complexes with DNA-binding ligands. *ChemBioChem*, **2005**, *6*, 414 – 421.

[111] - Haefliger, P.; Agorastos, N.; Renard, A.; Giambonini-Brugnoli, G.; Marty, C.; Alberto R. Cell uptake and radiotoxicity studies of an nuclear localization signal peptide-intercalator conjugate labeled with [$^{99m}\text{Tc}(\text{CO})_3$] $^+$. *Bioconjugate Chem.*, **2005**, *16*, 582 – 587.

[112] - Agorastos, N.; Borsig, L.; Renard, A.; Antoni, P.; Viola, G.; Spingler, B.; Kurz, P.; Alberto, R. Cell-specific and nuclear targeting with $[\text{M}(\text{CO})_3]^+$ ($\text{M} = ^{99m}\text{Tc}, \text{Re}$)-based complexes conjugated to acridine orange and bombesin. *Chem. Eur. J.*, **2007**, *13*, 3842 – 3852.

[113] - Vitor, R.F.; Correia, I.; Videira, M.; Marques, F.; Paulo, A.; Pessoa, J.C.; Viola, G.; Martins, G.G.; Santos, I. Pyrazolyl–diamine ligands that bear anthracenyl moieties and their rhenium(I) tricarbonyl complexes: synthesis, characterization and DNA-binding properties. *ChemBioChem*, **2008**, *9*, 131 – 142.

[114] - Vitor, R.F.; Esteves, T.; Marques, F.; Raposinho, P.; Paulo, A.; Rodrigues, S.; Rueff, J.; Casimiro, S.; Costa, L.; Santos I. ^{99m}Tc -Tricarbonyl Complexes Functionalized with Anthracenyl Fragments: Synthesis, Characterization and Evaluation of Their Radiotoxic Effects in Murine Melanoma Cells. *Cancer Biother. Radiopharm.*, *in press*.